Design of a Series of Polythiophenes Containing C60 Groups: Synthesis and Optical and Electrochemical Properties

ARTICLE *in* MACROMOLECULES · JANUARY 2015

Impact Factor: 5.8 · DOI: 10.1021/ma501788d

Macromolecules

Article

pubs.acs.org/Macromolecules

Design of a Series of Polythiophenes Containing C_{60} Groups: Synthesis and Optical and Electrochemical Properties

Lara Perrin,*[†,‡] Mathilde Legros,[†,‡] and Régis Mercier[‡]

[†]LEPMI, Univ. Savoie, F-73000 Chambéry, France

[‡]LEPMI, CNRS, F-38000 Grenoble, France

ABSTRACT: In order to develop polymers combining both acceptor and donor moieties, a series of alternating copolymers based on C_{60} fullerene and oligothiophenes were synthesized. First, a diamino-functionalized fullerene was obtained by a three-step modification of 4,4′-diaminobenzophenone, followed by a Bamford−Stevens addition on C_{60}. A series of oligo-3-alkylthiophenes O3AT, with various polymer and alkyl chains lengths, were synthesized using the Grignard metathesis method and dicarbonylated by Vilsmeier formylation. Alternating copolymers $[C_{60}\text{-O3AT}]_n$ were finally obtained by polycondensation, taking a specific care concerning synthesis conditions in order to optimize polymerization degrees. Nuclear magnetic resonance, infrared spectroscopy, gel permeation chromatography and thermogravimetric analysis were achieved in order to determine the structure of each copolymers. In addition, their functional properties (UV−vis absorption, photoluminescence, and electronic levels) were measured and related to the ascertained average compositions.

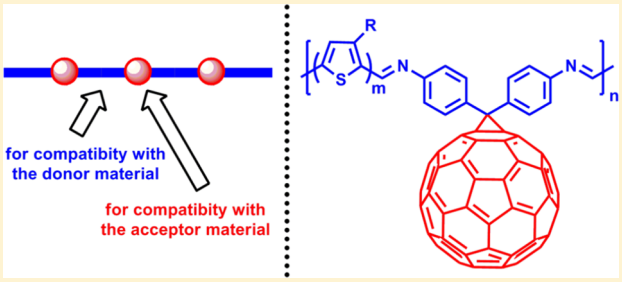

1. INTRODUCTION

First described in the 1970s,[1−3] organic photovoltaic (OPV) materials seem to be an interesting alternative to inorganic materials. More specifically, new "plastic" photovoltaic devices have a great potential for low cost, low weight, flexibility, and large-size processability.[4] Recent studies even light up their real potential for short energy payback time.[5] However, in order to become a real alternative to the inorganic technology, several challenges must be overcome including the low conversion efficiency and the rapid degradation of performance.

The active layer of organic solar cells usually consists of a blend of two materials: an electron-donor π-conjugated polymer D and an electron-acceptor fullerene derivative A. Bulk heterojunction devices based on poly(3-hexylthiophene) (P3HT) and [6,6]-phenyl-C_{61}-butyric acid methyl ester (PCBM) represent the most investigated system and can be considered as a reference structure with efficiencies up to 3−5%.[6,7] Higher performances around 9−11%[8−10] have already been reached using new low-band-gap polymers and tandem cell architectures.

The photovoltaic efficiencies and their long-term stability are, among other factors like the photoactive materials choice and device encapsulation, directly related to the morphology of the active layer.[11,12] Indeed, in a bulk heterojunction solar cell, the low miscibility between the acceptor and donor materials does not allow an optimization of the size of their domains. Furthermore, an unfavorable evolution of the morphology can occur after several running hours. In both cases, this results in a nonoptimized separation of charges in the D/A interpenetrating network. It is thus necessary to find a good compromise between the following characteristics: (i) a large surface of interface between the acceptor and donor phases to facilitate the excitons separation, (ii) a size of domains close to the length of excitons diffusion (3−20 nm[13−15]) in order to minimize the loss of charges by recombination but large enough to allow the excitons separation, and (iii) a thin active layer thickness (∼100−200 nm) in order to optimize the charge collection toward the electrodes.

Traditionally, morphology improvement can be realized during or after the active layer deposition through several ways: modification of the D/A ratio,[16,17] change of the solvent,[18] use of processing additives,[19−21] and vapor[22,23] or thermal[18,24] annealing treatments. In addition, the use of D−A copolymers as compatibilizing agent offers another especially interesting approach to improve or stabilize the morphology. As regards this latter strategy, several recent works[25−27] and reviews[28−31] report new structures incorporated as ternary components in photoactive layers with the aim of enhancing photovoltaic conversion or stabilizing device performance by control of the nanoscale morphology. Among materials that have demonstrated success, most of them are composed of two types of units with structures close to D and A active materials used. Introduced in the D/A blend system, these structures could find a place at the interphase. For instance, diblock[27,32,33] or brush[34] copolymers have demonstrated their potential for beneficial effect on morphology. However, the presence of

Received: August 29, 2014
Revised: December 19, 2014
Published: January 8, 2015

DOI: 10.1021/ma501788d
Macromolecules 2015, 48, 323−336

insulating parts unavoidable for the design of the C_{60} block can degrade the rate of recovered charges. Recently, the use of oligothiophene units grafted or end-capped by C_{60} units[35−38] also proved their aptitude to improve or stabilize OPV performances. Considering these interesting results, we were interested to develop longer patterns using alternating oligothiophene/C_{60} copolymers (Figure 1). Indeed, synthesis

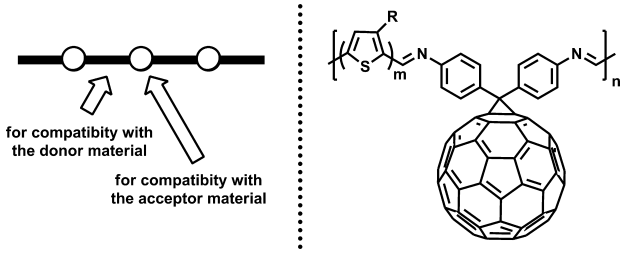

Figure 1. General structure of the copolymer family $[C_{60}\text{-O3AT}]_n$.

ways can be conducted in order to ensure minimal insulating linker between the active moieties. And, as already reported in the literature,[39,40] alternating or random copolymers could have a role to play as compatibilizing agents.

The present paper describes the synthesis method deployed to prepare a large variety of new linear and soluble oligothiophene/C_{60} alternating copolymers $[C_{60}\text{-O3AT}]_n$ as potential compatibilizing agents for P3HT/PCBM-based devices. The most reported procedures to access fullerene containing copolymers (alternating or random) are the following: polymers with pendant C_{60} fullerenes,[41−49] radical or Prato-based additions of a monomer on C_{60} fullerene,[50−55] and reaction of a bifunctional fullerene with another bifunctional monomer.[56] Among these possibilities, the latter strategy was chosen according to the interesting possibility to control both the minimization of the insulating linker and the absence of fullerene poly adducts derivatives. The minimization of the insulating linker is expected to ensure enhancement of the charges transfer and transport during the photovoltaic process. As regards the previous stage of fullerene difunctionalization to consider due to the ability of C_{60} to accept up to six electrons, this will undeniably help to obtain linear, un-cross-linked, and soluble copolymers.

In order to synthesize the alternating $[C_{60}\text{-O3AT}]_n$ copolymers presented in Figure 1, the chosen synthesis methodology was a polycondensation reaction involving a diamino fullerene $C_{60}\text{-NH}_2/\text{NH}_2$ and a dialdehyde oligothiophene O3AT-CHO/CHO. Thus, the first stage of the work was dedicated to the synthesis of both acceptor and donor difunctionalized monomers, each time completed by a careful stage of model syntheses in order to optimize the final condensation conditions. A series of copolymers were then synthesized using various alkyl and oligothiophene chains lengths. Their chemical structures were investigated using nuclear magnetic resonance (NMR), infrared spectroscopy (IR), gel permeation chromatography (GPC), and thermogravimetric analysis (TGA) and correlated to functional properties (UV−vis absorption, photoluminescence, and electronic levels).

2. RESULTS AND DISCUSSION

2.1. Acceptor Monomer. *2.1.1. Synthesis of a Diamino-Functionalized Fullerene: $C_{60}\text{-NH}_2/\text{NH}_2$.* Among possible fullerene diamino functionalization methods described in the literature,[57−60] the chosen derivative was a diaminophenyl-modified C_{60} (see compound **5** in Scheme 1). The structure of this derivative will allow a π-conjugated extension of the linked donor unit, and its synthesis is accessible in four steps (Scheme 1).[60]

In a first step, the amino groups of 4,4′-diaminobenzophenone were protected by amido conversion using trifluoroacetic anhydride. This protected compound was then transformed in a diazo derivative by condensation with *p*-tosylhydrazide. After that, the deprotection of amino groups was realized in basic media. In order to confirm the entire success of the deprotection, the reaction was monitored by ^{19}F NMR analysis until extinction of the $-CF_3$ characteristic signal at −76.21 ppm. Surprisingly, two different solid compounds could be then isolated at this step: a white precipitate in the reaction mixture and a yellow solid obtained after treatment of the aqueous reaction media (solvent extraction and concentration by evaporation). ^{13}C NMR spectra of both compounds were quite similar and compatible with compound **4**, while ^{1}H NMR spectra were really different (absence of the ═N−NH− signal for the precipitate and significant shifts for the aromatic and amine signals). Complementary analyses were realized by mass

Scheme 1. Synthesis of the Acceptor Monomer $C_{60}\text{-NH}_2/\text{NH}_2$

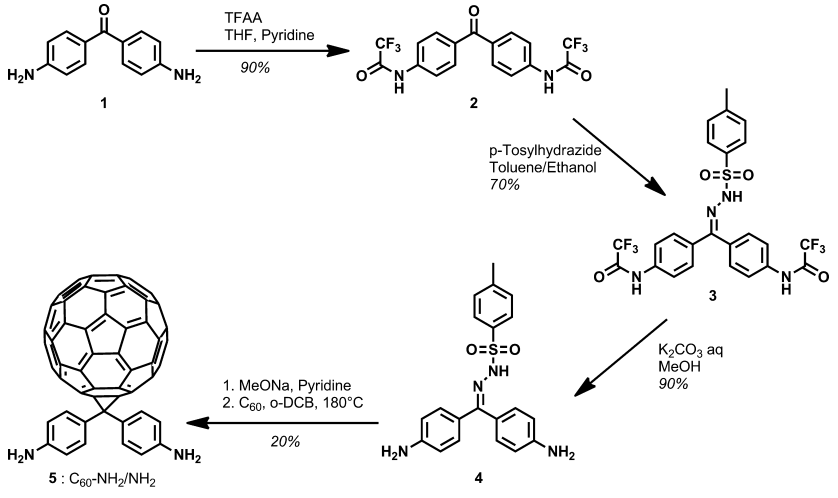

DOI: 10.1021/ma501788d
Macromolecules 2015, 48, 323−336

Scheme 2. Synthesis of Two Model Triads T_m-C_{60}-T_m

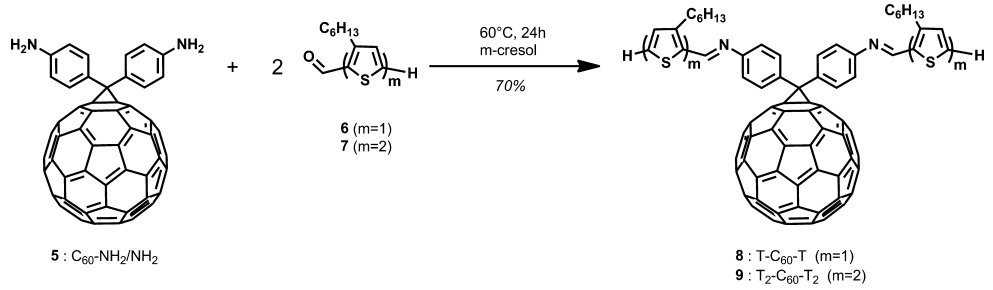

spectrometry (ESI-TOF), and the same major m/z signal, compatible with $[M + H]^+$ of **4**, was observed for both compounds. The additional presence of the $[M + K]^+$ signal only in the case of the white solid suggests that it corresponds to a ionic salt form (K^+, $-^-N-N=$). Furthermore, this ionic form could be converted into the corresponding protonated compound by passing through a silica gel column (known to be weakly acid).

The last reaction step was the addition of the previous hydrazone on C_{60} according to a 1,3-dipolar cycloaddition mechanism using the Bamford–Stevens method to afford the C_{60}-NH_2/NH_2 derivative **5**. The overall yield after the four steps reaction was around 11%. ^{13}C NMR analysis indicates the formation of only the [6–6]-closed fullerene isomer.[61] Indeed, under high reaction temperature, the [5–6]-open isomer can undergo conversion to the [6–6]-closed isomer which is more thermodynamically stable.[62] Even after a long drying period at 100 °C under vacuum, the final product always contains some residual toluene. This residual toluene signal may have probably misled previous literature ^1H NMR interpretation.[60]

2.1.2. Synthesis of Two Model Triads: T_m-C_{60}-T_m. In order to validate the reactivity of the low soluble C_{60}-NH_2/NH_2 derivative in future amine/aldehyde condensations, two model triads based on thiophene were synthesized. In addition, the ^1H NMR signature of these model triads will undeniably clarify future copolymers spectra. Scheme 2 illustrates the general procedure used for the synthesis of model triads.

Initially, 3-hexylthiophene-2-carbaldehyde (**6**) and 3,3′-dihexyl-2,5′-bithiophene-2-carbaldehyde (**7**) reagents were synthesized in the laboratory using procedures close to those reported in the literature.[63,64] Then, both aldehyde compounds were involved in a condensation reaction with the diamino-functionalized fullerene C_{60}-NH_2/NH_2 affording respectively T-C_{60}-T (**8**) and T_2-C_{60}-T_2 (**9**) triads with a 70% yield after purification.

As shown in Figure 2, the structure of each triad was confirmed by ^1H NMR analysis. The characteristic signal of Schiff bases (–CH=N–) was identified at 8.6 ppm, thus indicating the success of the condensation reaction. The two doublets at 8.1 and 7.3 ppm, observed for both triads, are attributed to the phenyl groups carried by the C_{60} fullerene moiety. The characteristic signature of thiophenic protons can also be observed in Figures 2a and 2b corresponding to thiophene and bithiophene units, respectively.

2.2. Donor Monomer. *2.2.1. Synthesis of a Dicarbonylated Oligo-3-alkylthiophenes Series: O3AT-CHO/CHO.* In order to elaborate a series of regioregular oligo-3-alkylthiophenes with controlled length, the Grignard metathesis (GRIM) method[65] was chosen. This method can be carried out at ambient temperature and allows easy control of the

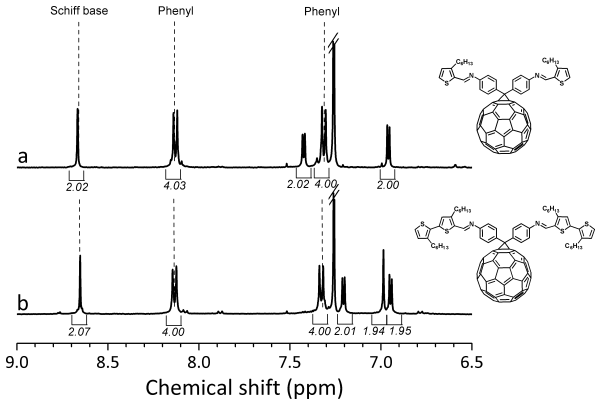

Figure 2. ^1H NMR spectra of the two model triads T_m-C_{60}-T_m (400 MHz, $CDCl_3$, zoom on aromatic signals, real integration values are given in italics, the cut signal corresponds to the NMR solvent).

polymerization degree by modulation of the monomer/catalyst ratio.[66,67] This polymerization method is based on a Kumada coupling that occurs under the action of a catalyst (Ni or Pd) and involves a halogenated compound and an organometallic initiator.

The aim was to study both the influence of the alkyl chain and polymer chain lengths. Thus, three different alkylated thiophene monomers (hexyl, octyl, and decyl) were initially prepared. As presented in Scheme 3, the polymerization was realized using 2-bromo-5-iodothiophene monomers (**10**) in order to obtain regiospecific magnesium intermediates and highly regioregular polythiophenes.[65]

As regards the synthesis of initial 2-bromo-5-iodothiophene reagents, a specific care was taken in order to obtain high purity compounds. In an initial approach, the iodation of 2-bromothiophene derivatives was realized using *N*-iodosuccinimide.[68] This synthesis method was not enough regioselective to reach adequate purity. Therefore, a iodation using the combination of iodine and iodobenzene diacetate[65] was used. After Kugelrohr distillation, the aimed compounds **10** were obtained with purities greater than 98% (determined by gas chromatography/mass spectrometry).

As shown in Scheme 3, the synthesis of dicarbonylated oligo-3-alkylthiophenes was conducted in two main stages: the chain growth polymerization and the formylation of end-chain units. The polymerization was conducted according to a four-step procedure. First, the thiophene monomer is activated in position 5 by the action of *tert*-butylmagnesium chloride Grignard reagent. Second, the chain growth occurs at room temperature under the action of 1,3-bis(diphenylphosphino)-propane nickel(II) chloride catalyst ($[Ni(dppp)Cl_2]$). After 4 h, the polymerization is quenched by addition of an HCl aqueous

DOI: 10.1021/ma501788d
Macromolecules 2015, 48, 323–336

Scheme 3. Synthesis of a Series of Donor Macromonomers O3AT-CHO/CHO

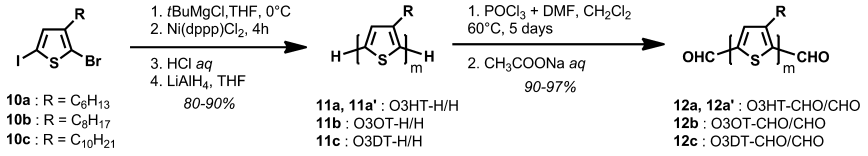

solution in order to favor low dispersities.[69] At this step, an additional reduction of dispersities was achieved using Soxhlet fractionation with methanol, petroleum ether, and chloroform. Dispersities $Đ$ measured by gel permeation chromatography (solvent THF, 25 °C) were between 1.3 and 1.6 for all selected oligothiophene fractions. Afterward, the oligothiophenes series was debrominated by action of the lithium aluminum hydride in order to prepare the formylation. The success of this step was checked by MALDI-TOF mass spectrometry showing the disappearance of m/z characteristic signals corresponding to H/Br end groups in favor of m/z characteristic signals of H/H end groups.

Lastly, the series of oligothiophenes was difunctionalized by aldehyde functions via the Vilsmeier−Haack reaction (Scheme 3). This reaction has already proved reliable results on polythiophene difunctionalization in the literature.[70,71] The end-functionality was evaluated by both MALDI-TOF mass spectrometry (m/z characteristic signals for CHO/CHO end groups) and ^{1}H NMR spectroscopy (Figure 3).

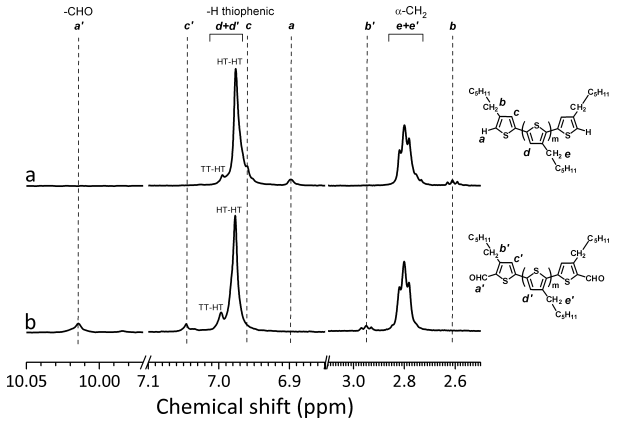

Figure 3. ^{1}H NMR spectra of oligothiophenes (400 MHz, $CDCl_3$, zoom on the different end-chain characteristic signals): (a) O3HT-H/H; (b) O3HT-CHO/CHO (also given the thiophene units arrangement using H for head and T for tail).

As shown in Figure 3, the success of the dialdehyde functionalization was confirmed by ^{1}H NMR analysis. Indeed, the CHO functionalization is evidenced by the presence of the aldehyde signal at 10.01 ppm. Moreover, the disappearance or shift of small signals attributed to aromatic and aliphatic end-chain protons indicates the quite overall end-functionalization. The more significant shift (2.61 to 2.95 ppm) concerns the triplet attributed to α-CH_2 of end-chain thiophene units. All other signals attributions are represented on Figures 3a and 3b, in accordance with literature reported interpretations.[54,70,72]

Proton NMR analyses conducted on the dicarbonylated oligo-3-alkylthiophenes series evidence a relative good end difunctionalization of all macromononomers. According to MALDI-TOF mass spectra, the presence of monofunctionalized derivatives O3AT-CHO/H can be sometimes detected in addition to O3AT-CHO/CHO characteristic m/z mass signals. However, according to the good recovery of proton integrations in the three new signals (a′, b′, and c′) compared to missing initial signals (a and b) with a standard deviation lower than 5%, it can be assumed that the degree of aldehyde end-functionalization is about 95−100%.

The oligothiophene regioregularity RR can also be evaluated by ^{1}H NMR. The degree of RR is defined as the fraction of monomers adopting a head-to-tail (HT) configuration, rather than other arrangements. According to Barbarella et al.,[73] identification of NMR shifts (see Figure 3), the regioregularities of the oligothiophene series were estimated to be always higher than 90%.

Four different oligothiophenes O3AT were synthesized according to the preceding procedure. The choice was guided by the two following objectives: (i) study of the impact of the alkyl chain length with the synthesis of three oligo-3-alkylthiophenes having close molecular weights and different alkyl chains: hexyl, octyl, and decyl for **12a**, **12b**, and **12c**, respectively; (ii) study of the impact of the polymer chain length with two oligo-3-hexylthiophenes having two different molecular weights: **12a** and **12a′** with a targeted polymerization degree of 30 and 15 units, respectively.

As shown in Figure 4, the GPC chromatograms of the four synthesized O3AT oligomers indicate similar elution volumes

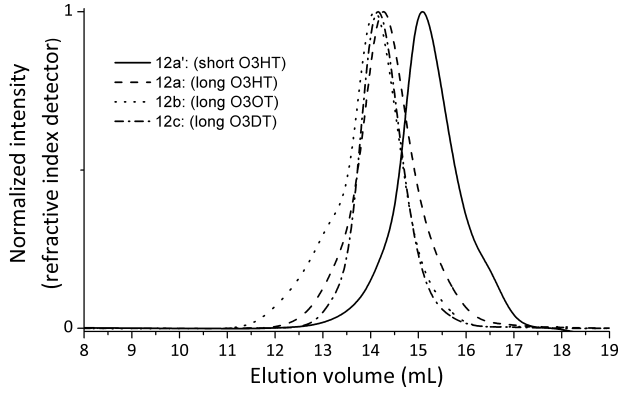

Figure 4. GPC chromatograms of donor oligothiophene monomers O3AT (conditions: THF, 25 °C).

for **12a**, **12b**, and **12c** derivatives and lower value for **12a′**. The corresponding number-average molecular weights (M_n) are presented in Figure 5. Nevertheless, one major issue in this work was to find a convenient way to estimate the real molecular weights of O3AT donor units. Indeed, the GPC method used relies on a calibration using polystyrene standards which implies a difference with the true molecular weight.[74] (It should be mentioned that the absolute molecular weight determination GPC method using light scattering is not suitable for thiophene-based polymers due to their luminescence properties.)

DOI: 10.1021/ma501788d
Macromolecules 2015, 48, 323−336

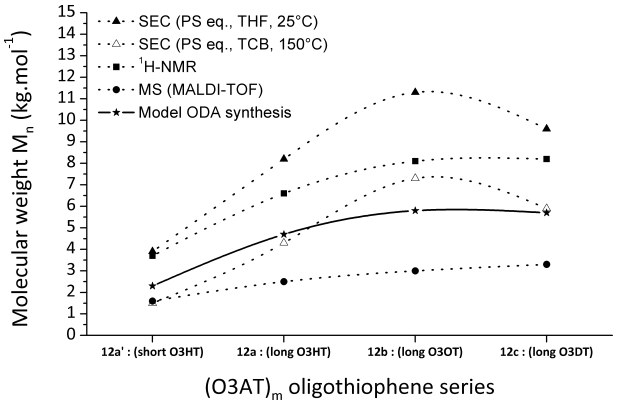

Figure 5. Molecular weights estimation of donor macromonomers (O3AT) using different methods (lines are a guide to the eyes).

In order to optimize the final C_{60}/O3AT polycondensation reaction, it is necessary to know the molecular weight of each monomer unit used with an adequate precision. Indeed, the copolymer molecular weight will be directly linked to the NH_2/CHO functional units ratio (equivalent to the C_{60}/O3AT ratio), which should be as close as possible to 1.

Figure 5 presents the molecular weights estimation of O3AT monomers using five different methods. First of all, four traditional methods were compared: room temperature GPC, high temperature GPC, proton NMR, and MALDI-TOF mass spectrometry. For GPC measured values, a significant difference is observed between measurements realized either at 25 °C in tetrahydrofuran (THF) or at 150 °C in 1,2,4-trichlorobenzene (TCB): diminution of a factor close to 1.5−1.9 for long O3AT and 2.6 for short O3AT. According to the literature,[75] polythiophenes adopt a rodlike conformation in solution leading to a GPC overestimation of molecular weights when compared to polystyrene. This overestimation is less important in TCB as the solubility and mobility are increased by both solvent and temperature. ^{1}H NMR estimations could also result in an overestimation increasing with the molecular weight because the calculation is realized using a very weak end-chain NMR signal (see protons *b* and *e* in Figure 3), thus giving a measurement uncertainty. As regards MALDI-TOF, M_n values (obtained by the statistical average method) are significantly lower than the others. This difference between GPC and MALDI-TOF measurements was also observed by Lui et al., with a stronger difference when M_n increase.[76] However, these latter values should also be used with caution as the desorption/ionization phenomena in mass spectrometry could be more favorable to lower molecular weight chains.[77,78]

In order to determine more precisely the optimal quantity of O3AT-CHO/CHO oligomer required to obtain a NH_2/CHO ratio close to 1, a model polycondensation series introducing a substitution diamine was realized. The 4,4′-oxidianiline (ODA) was chosen due its commercial availability and structure close to the C_{60}-NH_2/NH_2 acceptor monomer.

2.2.2. Synthesis of a Model Copolymers Series: [ODA-O3AT]$_n$. Scheme 4 presents the general synthesis route executed with a series of ODA/O3AT weight ratio for each selected O3AT monomers. The polycondensation was realized in a mixture of THF/DMF (6/2), an aprotic solvent shared by O3AT, ODA, and C_{60}-NH_2/NH_2 monomers. To favor the condensation mechanism, the reaction was thermally activated and acid-catalyzed using *p*-toluenesulfonic acid (PTSA) in the presence of calcium chloride in order to remove produced water from the reaction media.

For the four selected O3AT monomers, a series of polycondensation reactions were realized by varying the ODA/O3AT weight ratio (minimum six ratios chosen between GPC and MALDI-TOF number-average molecular weight estimations). Figure 6 shows examples of ^{1}H NMR profiles for

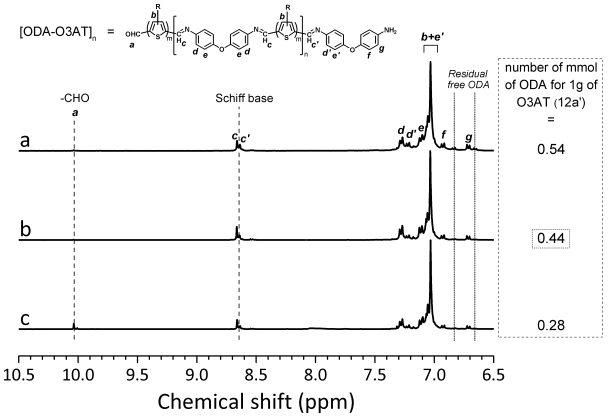

Figure 6. ^{1}H NMR spectra of different [ODA-(short O3HT)]$_n$ synthesis batches (NMR conditions: 400 MHz, $C_2D_2Cl_4$, 70 °C).

the crude reaction products (spectra are normalized on the signal of thiophenic *b* protons). The low solubility of obtained copolymers did not allow complete GPC analyses of crude samples. Thus, the optimal polycondensation conditions were determined according to NMR analyses. Indeed, it could be considered that the ODA/O3AT ratio is close to the optimum when the signal due to the Schiff base is maximal (see signal *c* in Figure 6) and that signals due to initial monomers or end units are minimal (protons *a*, *c*′, *d*′, *e*′, *f*, *g* and free ODA). As shown in the example presented in Figure 6b, the selected ratio was 0.44 mmol of ODA per gram for the short O3HT (**12a**′), value equivalent to 0.88 mmol of CHO functions. To illustrate the success of the polymerization, values given by GPC analysis of the chloroform soluble fraction of this copolymer were M_n = 17 500 and $Đ$ = 3 (conditions: THF, 25 °C, PS equiv), corresponding to an average repetition of 4−5 units.

The number of aldehyde equivalents per gram of O3AT was determined for the four selected oligothiophenes according to the same NMR identification process, and the issues are presented in Table 1. The estimated polymerization degrees of

Scheme 4. Synthesis of a Model Copolymers Series [ODA-O3AT]$_n$

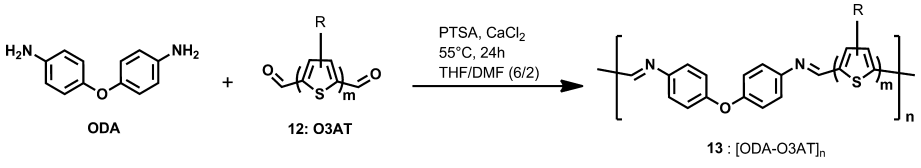

DOI: 10.1021/ma501788d
Macromolecules 2015, 48, 323−336

Table 1. O3AT-CHO/CHO Characteristics Selected for the $[C_{60}\text{-O3AT}]_n$ Copolymers Syntheses

	aldehyde equivalents (mmol)/g of oligothiophene
12a′: $(HT)_{13}$	0.880
12a: $(HT)_{28}$	0.424
12b: $(OT)_{30}$	0.344
12c: $(DT)_{25}$	0.352

O3AT monomer units are also indicated using the following nomenclature: $(AT)_m$ with A the nature of the alkyl chain and m the average number of thiophene T repeating units determined using the model copolymerization with ODA. As shown in Figure 5, the corresponding M_n values were intermediate to other determination methods used and close to high temperature GPC values.

2.3. Conception of a Series of Oligothiophene/Fullerene Alternating Copolymers. *2.3.1. Synthesis and Purification of the $[C_{60}\text{-O3AT}]_n$ Copolymers.* As shown in Scheme 5, the synthesis route used for the C_{60}/O3AT copolymers was similar to the previous ODA/O3AT copolymers synthesis. The C_{60}/O3AT molar ratios introduced were close to one, and the corresponding weight amounts were calculated according to Table 1 using the same O3AT synthesis batches as for the model ODA copolymers syntheses.

In order to reduce the impact of the sterical hindrance brought by fullerene moieties, a reaction time of 7 days was applied. Each $[C_{60}\text{-O3AT}]_n$ polymer synthesis was then followed by a purification and fractionation using Soxhlet extraction with methanol, hexane, chloroform, and *o*-dichlorobenzene, sequentially. For each synthesis, two fractions could be isolated: $CHCl_3$ (chloroform soluble) and *o*-DCB (*o*-dichlorobenzene soluble). Each time, a non-negligible fraction of insoluble material was also produced.

2.3.2. Determination of the Chemical Structure of $[C_{60}\text{-O3AT}]_n$ Copolymer Fractions. The success of the polycondensation reaction was confirmed by both IR and NMR spectroscopies. The characteristic IR signal for an imine (C═N stretching vibration mode) was identified at 1650 cm^{-1}, and the NMR characteristic signal of Schiff bases (−CH═N−) was identified at 8.7 ppm.

As shown in the ^1H NMR examples presented in Figure 7, all expected signals were identified. Nevertheless, some signals due to end-chain units were also represented, suggesting a weak polymerization degree. In particular, the characteristic signal of aldehyde functions (−CHO) was present in all fractions. In addition, some fractions were also more or less rich in C_{60} characteristic end-units (generally *o*-DCB fractions were richer than their $CHCl_3$ counterparts; see Figure 7).

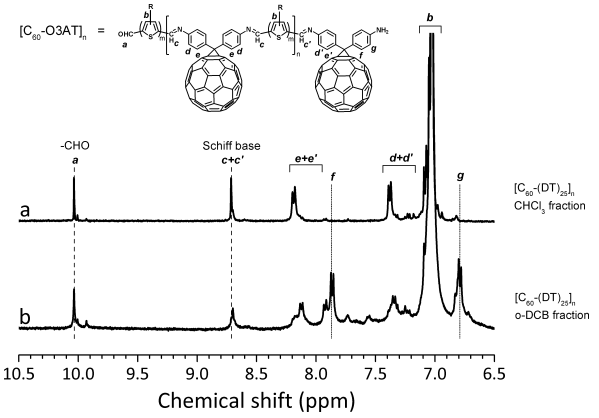

Figure 7. ^1H NMR spectra of the different Soxhlet fractions for the $[C_{60}\text{-}(DT)_{25}]_n$ synthesis batch: (a) chloroform extraction; (b) *o*-dichlorobenzene extraction (NMR conditions: 400 MHz, $C_2D_2Cl_4$, 70 °C).

Figure 8 shows the GPC chromatogram of the chloroform soluble fraction of the $[C_{60}\text{-}(AT)_{13}]_n$ copolymer. When

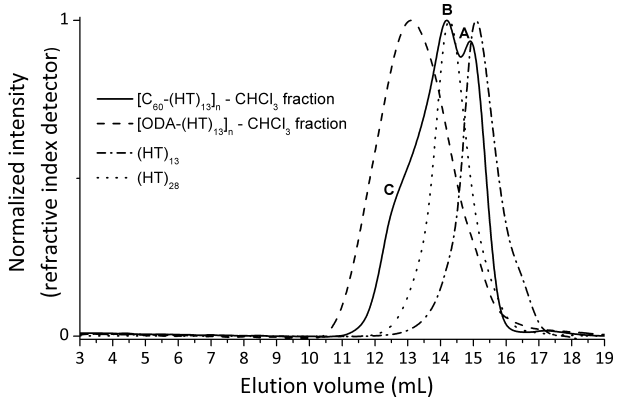

Figure 8. GPC chromatograms of fractions soluble in $CHCl_3$ for both C_{60} and ODA copolymers based on $(HT)_{13}$, compared to $(HT)_{13}$ and $(HT)_{28}$ oligothiophene monomers (GPC conditions: THF, 25 °C).

compared to its ODA copolymer equivalent, it is obvious that the polycondensation was less efficient and less homogeneous when using the C_{60} derivative. Nevertheless, considering that the GPC contribution of a C_{60} unit is weak,[79] the comparison with $(HT)_{13}$ and $(HT)_{28}$ oligothiophene monomers chromatograms allows to qualitatively assign the three observed shoulders. The shoulder A can be composed of C_{60}-O3HT diads and C_{60}-O3HT-C_{60} triads with possible residual O3HT. The shoulder B probably consists in a copolymer chain composed of two O3AT patterns with

Scheme 5. Synthesis of the Alternating A−D Copolymers Series $[C_{60}\text{-O3AT}]_n$

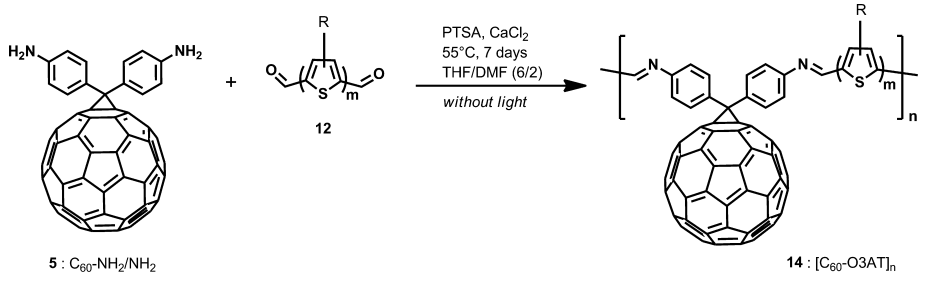

DOI: 10.1021/ma501788d
Macromolecules 2015, 48, 323−336

between 1 and 3 fullerene units. The shoulder C is made of copolymer chains composed of three or more O3AT patterns.

The molecular weight estimation given by high temperature GPC for the different $[C_{60}\text{-O3AT}]_n$ copolymers fractions is presented in Table 2. The molecular weights of their initial O3AT building blocks, determined in the same analyses conditions, are also presented for comparison. It can be thus concluded that the average polymerization degree is probably close to 2. This weak value can be a consequence of the copolymers limited solubility in the reaction media. Moreover, a high fraction of insoluble materials was always collected meaning that higher polymerization degrees should lead to insoluble copolymers.

Table 2. Molecular Weights of the Different $[C_{60}\text{-O3AT}]_n$ Soxhlet Fractions, with the Corresponding O3AT Macromonomers Analyzed in the Same GPC Conditions (Trichlorobenzene, 150 °C, PS equiv)

	$[C_{60}\text{-O3AT}]_n$ copolymers		O3AT monomers	
	M_n	Đ	M_n	Đ
$[C_{60}\text{-(HT)}_{13}]_n$ $CHCl_3$ fraction	4200	2.2	1500	3.2
$[C_{60}\text{-(HT)}_{28}]_n$ $CHCl_3$ fraction	7600	2.6	4300	2.0
$[C_{60}\text{-(OT)}_{30}]_n$ $CHCl_3$fraction	11700	3.5	7300	1.9
$[C_{60}\text{-(OT)}_{30}]_n$ *o*-DCB fraction	15800	2.4	7300	1.9
$[C_{60}\text{-(DT)}_{25}]_n$ $CHCl_3$ fraction	10300	2.1	5900	1.5
$[C_{60}\text{-(DT)}_{25}]_n$ *o*-DCB fraction	13300	3.6	5900	1.5

Synthesized copolymers were also characterized by thermogravimetric analysis (TGA). All copolymer fractions present a degradation temperature close to 400 °C, like their initial oligothiophene building blocks. As shown in Figure 9, the C_{60} fullerene part does not undergo degradation until 700 °C. Therefore, TGA thermograms can help to confirm the composition of the copolymers fractions. Associated with NMR and GPC previous results, it can be thus generally concluded that the average composition of majority $[C_{60}\text{-O3AT}]_n$ chains should be the following: (i) $CHCl_3$ Soxhlet fractions: O3AT-C_{60}-O3AT and (ii) *o*-DCB Soxhlet fractions: C_{60}-O3AT-C_{60}-O3AT-C_{60}.

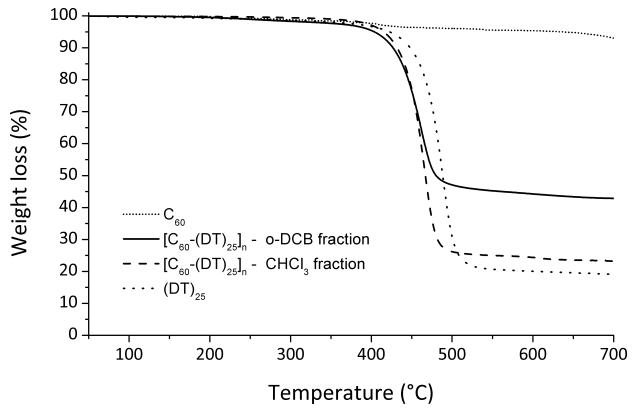

Figure 9. TGA thermograms of the different Soxhlet fractions for the $[C_{60}\text{-(DT)}_{25}]_n$ copolymer compared to the $(DT)_{25}$ initial oligothiophene monomer and to C_{60} (under a nitrogen atmosphere).

2.4. Optical Properties. *2.4.1. T_m-C_{60}-T_m Model Triads.* Figure 10 presents the UV−vis absorption spectra in chloroform of both synthesized model triads (**8** and **9**). The fullerene pattern exhibits three absorption peaks: the characteristic C_{60} moiety absorption at 280 and 330 nm[80] and a weak peak at 700 nm, specific for methanofullerene compounds.[44] As regards the contribution of the phenyl−thiophene π-conjugated systems, the spectrum of T_2-C_{60}-T_2 triad clearly reveals the phenyl−bithiophene absorption band at around 375 nm. In the case of the T-C_{60}-T triad, the absorption contribution of the less extended π-conjugated phenyl−thiophene system is evidenced by a slight shoulder at 360 nm.

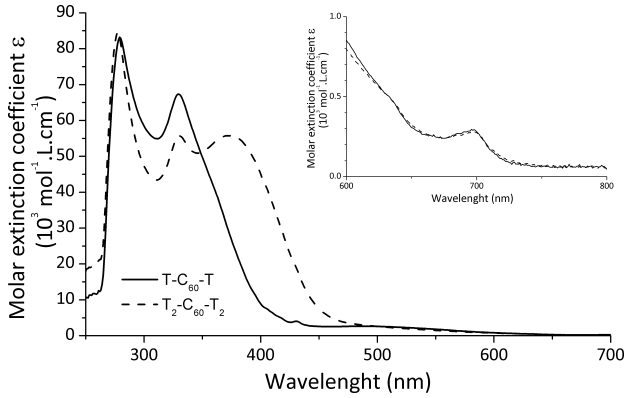

Figure 10. UV−vis absorption spectra of the two model triads T_m-C_{60}-T_m (1.5×10^{-4} M in chloroform). The inset highlights a very weak characteristic absorption band of the fullerene moiety.

The UV−vis absorption spectra of these model triad systems consist of a superposition of the spectra of each units separated by a nonconjugated linkage. This is in accordance with other similar systems described in the literature.[81−84]

2.4.2. $[C_{60}\text{-O3AT}]_n$ Copolymers. Figure 11 presents the UV−vis absorption spectra in *o*-dichlorobenzene of the different $[C_{60}\text{-O3AT}]_n$ copolymer fractions isolated. The spectra of all samples consist of the superposition of the C_{60} fullerene (330 nm) and π-conjugated chain (about 460 nm for all O3AT monomers and copolymers) absorptions, similarly to model triads and other existing C_{60}−polythiophene linked systems.[85]

As shown in Figures 11a and 11b, two different behaviors were observed depending on the Soxhlet fraction of the copolymers. For the considered samples, $CHCl_3$ soluble fractions show quite similar UV−vis traces, and no influence of the alkyl/polymer chain lengths was detected on the maximum and edge wavelengths. When considering *o*-DCB soluble fractions, all samples also show quite similar UV−vis traces with an important reduction of the O3AT/C_{60} optical density ratio in comparison with $CHCl_3$ soluble fractions. The decrease of the mass extinction coefficient ε corresponding to the oligothiophene moiety was quantified to be about 30% between $CHCl_3$ and *o*-DCB Soxhlet fractions (Table 3). This observation is consistent with the previously considered average compositions of copolymer fractions.

Figure 12 presents the comparison between optical absorption spectra recorded from solution and solid film states for the different Soxhlet fractions of one $[C_{60}\text{-(AT)}_m]_n$ copolymer example. Corresponding data obtained for all synthesized copolymers are summarized in Table 3. First of

DOI: 10.1021/ma501788d
Macromolecules 2015, 48, 323−336

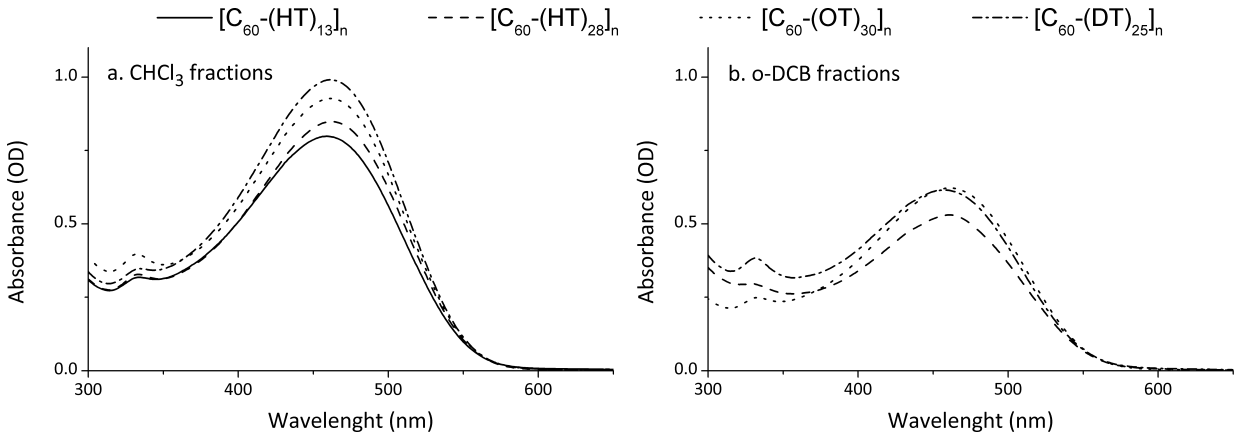

Figure 11. UV−vis absorption spectra of the $[C_{60}\text{-}(AT)_m]_n$ different Soxhlet fractions (0.1 mg/mL in *o*-dichlorobenzene).

Table 3. Optical Properties of Synthesized Copolymers

	solution[a]			film[b]		
copolymers	ε (L g^{-1} cm^{-1})	λ_{max} (nm)	Φ_{copo}/Φ_{oligo}[c]	λ_{max} (nm)	λ_{onset} (nm)	E_g^{opt}[d] (eV)
$[C_{60}\text{-}(HT)_{13}]_n$ $CHCl_3$ fraction	40	459	0.50	513	644	1.93
$[C_{60}\text{-}(HT)_{28}]_n$ $CHCl_3$ fraction	42	463	0.51	518	648	1.91
$[C_{60}\text{-}(HT)_{28}]_n$ *o*-DCB fraction	27	461	0.39	503	646	1.92
$[C_{60}\text{-}(OT)_{30}]_n$ $CHCl_3$ fraction	46	462	0.66	521	652	1.90
$[C_{60}\text{-}(OT)_{30}]_n$ *o*-DCB fraction	31	461	0.56	509	650	1.91
$[C_{60}\text{-}(DT)_{25}]_n$ $CHCl_3$ fraction	50	461	0.88	520	650	1.91
$[C_{60}\text{-}(DT)_{25}]_n$ *o*-DCB fraction	31	457	0.74	507	643	1.93

[a]Measured on *o*-dichlorobenzene solutions. [b]Observed with films casted from *o*-dichlorobenzene solutions on quartz plates. [c]The value given for Φ_{copo}/Φ_{oligo} corresponds to the fluorescence quantum yield reduction observed for $[C_{60}\text{-}(AT)_m]_n$ copolymers compared to the corresponding oligothiophene macromonomer measured in the same conditions ($\lambda_{excitation}$ = 460 nm). [d]The optical band gap was estimated in film using the formula $1240/\lambda_{onset}$.

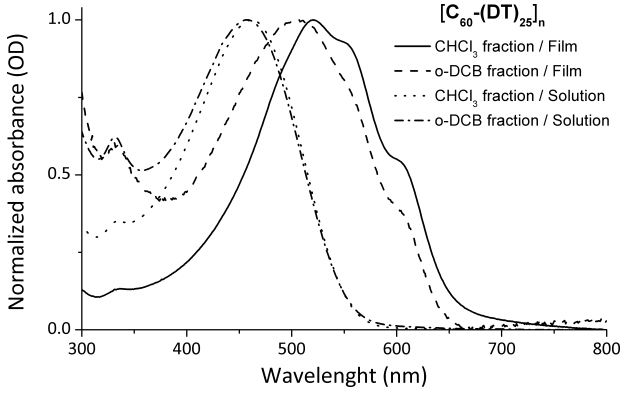

Figure 12. Comparison of solution and solid state UV−vis absorption spectra for the different fractions of the $[C_{60}\text{-}(DT)_{25}]_n$ copolymer.

all, an important red-shift and enlargement of the main peak are noticed on solid state spectra (difference of about 40−60 nm for λ_{max} and 90−100 nm for λ_{onset}). This phenomenon is attributed to conformation changes from the solution to the solid film state. In addition, a vibrational fine structure (shoulders) can be observed in solid state films, which is characteristic of the existence of π-stacking interactions. Second, the absorption spectra in film of *o*-dichlorobenzene Soxhlet fractions show a less pronounced bathochromic shift than their corresponding chloroform Soxhlet fractions (difference around 15 nm for λ_{max} and 5 nm for λ_{onset}). This means that the organization is disturbed either by the presence of more fullerene units or by the rigid imino linkage between oligothiophene units. However, the optical band gaps E_g^{opt} of all $[C_{60}\text{-}(AT)_m]_n$ copolymers fractions are close to 1.90 eV like for the initial $(AT)_m$ macromonomers (Table 3).

According to UV−vis absorption data, no significant interaction in the ground state was observed between oligothiophene and fullerene chromophores. On the other hand, both chromophores markedly interact in the excited state (Figure 13). Indeed, the copolymers emission spectra are

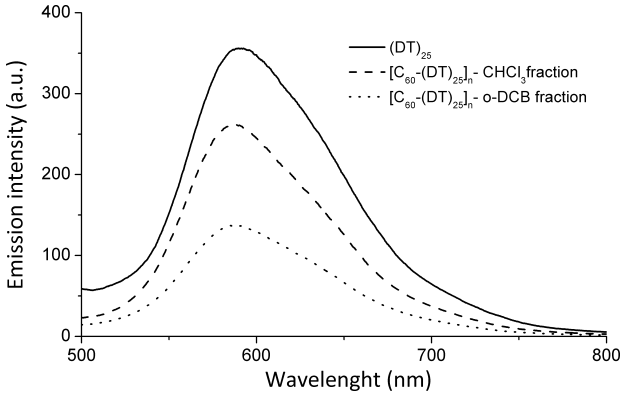

Figure 13. Fluorescence spectra of the $[C_{60}\text{-}(DT)_{25}]_n$ copolymer different fractions compared to the initial $(DT)_{25}$ oligothiophene macromonomer (2×10^{-4} mg/mL in *o*-dichlorobenzene, $\lambda_{excitation}$ = 460 nm).

characterized by a reduction of fluorescence when the oligothiophene chromophore is excited ($\lambda_{excitation}$ = 460 nm, $\lambda_{emission}$ ~ 590 nm for all copolymers and their initial macromonomers). Analyses were conducted in *o*-dichlorobenzene, using very diluted concentrations (~2×10^{-4} mg/mL) in order to minimize interchain transfers. Table 3 presents the reduction factor of fluorescence quantum yields observed between initial pristine O3AT units and O3AT units involved in a $[C_{60}\text{-O3AT}]_n$ copolymer (Φ_{copo}/Φ_{oligo}). A stronger quenching was observed for *o*-DCB Soxhlet fractions when

DOI: 10.1021/ma501788d
Macromolecules 2015, 48, 323−336

compared to their $CHCl_3$ Soxhlet fractions counterparts, these fractions being richer in C_{60} according to previously determined average compositions.

In the same condition of concentration, the O3AT fluorescence quantum yields were not affected when mixed with free fullerene in 1/1 or 1/2 molar ratio (the more soluble PCBM derivative was taken in order to ensure complete dissolution). This indicates that an efficient photoinduced intramolecular transfer take place from the oligothiophene unit to the fullerene unit in the case of copolymers, due to the fact that they are closely linked. A similar phenomenon has already been observed in the literature[81,85−87] in the case of oligothiophene−C_{60} diads or triads.

2.5. Electronic Energy Levels. *2.5.1. T_m-C_{60}-T_m Model Triads.* Figure 14 presents the cyclic voltammograms (CV) of

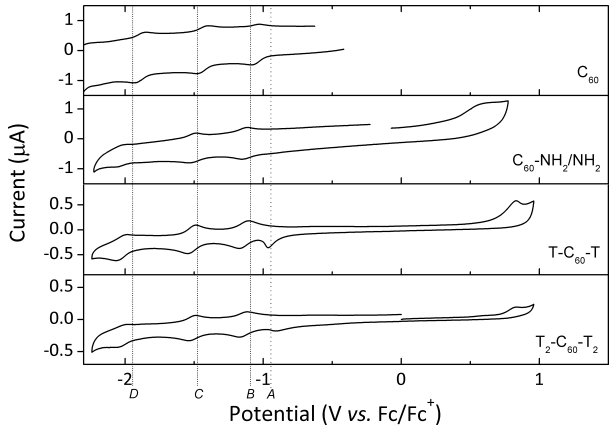

Figure 14. Cyclic voltammograms of the C_{60} fullerene, the intermediate derivative C_{60}-NH_2/NH_2, and the two model triads T-C_{60}-T and T_2-C_{60}-T_2 (10^{-4} M solutions in *o*-DCB/CH_3CN: 95/5).

both T-C_{60}-T and T_2-C_{60}-T_2 model triads compared to the pristine C_{60} fullerene and to the diaminophenyl-functionalized fullerene precursor C_{60}-NH_2/NH_2.

Concerning positive potentials, one irreversible oxidation peak was detected for the three functionalized fullerene derivatives. The fullerene C_{60} is known to be very difficult to be oxidized,[88,89] and no electrochemical oxidation could be observed with the experimental conditions for pristine C_{60}. Observed oxidation answers are thus attributed to linked moieties, i.e., aminophenyl, iminophenylthiophene, or bithiophene with onset potentials at respectively +0.35, +0.66, and +0.68 eV vs Fc/Fc^+. The replacement of the thiophene unit by a bithiophene shows no significant impact on the associated HOMO level (∼−5.5 eV, see Table 4).

As regards negative potentials, three reversible reductions waves were observed for the three functionalized fullerene derivatives (pointed out by the letters B, C, and D in Figure 14). Theses reductions are attributed to the C_{60} moiety and are very close to the corresponding ones of pristine C_{60} with a slight negative shift of about 0.10 eV. This little change is due to the more difficult reduction of the fullerene moiety after functionalization (loss of one double bond).[89] An additional irreversible peak (pointed out by the letter A in Figure 14) was also observed in the case of T_m-C_{60}-T_m triads. This peak of unknown origin has also been previously detected by Cravino et al.[90] in the case of a polythiophene with pendant C_{60} moieties. In both T_m-C_{60}-T_m triads, this peak could be observed on CV measurements realized either in solution or on films at onset potentials around −0.90 and −0.50 eV vs Fc/Fc^+ for respectively solution and film analyses (Figures 14 and 15). Furthermore, as shown in Figure 15, it was noticed that this additional irreversible peak was observed only in the case of previous scanning of positive potentials up to the region corresponding to the oxidation peak related to moieties linked to C_{60}. Thus, it could be concluded that the reduction answer A is related to the phenyl−thiophene pattern grafted on C_{60}. Considering the above-mentioned particularity of this peak, the LUMO energy levels of triads were estimated using the reduction onset of peak B (Table 4).

2.5.2. $[C_{60}$-O3AT$]_n$ Copolymers. Table 4 presents CV data of the different Soxhlet fractions of synthesized $[C_{60}$-O3AT$]_n$ copolymers; each time values related to the corresponding

Table 4. Electronical Properties (Reduction and Oxidation Potentials, LUMO and HOMO Energy Levels) of Synthesized Compounds

compounds	E_{onset}^{RED} [a] (V) vs Fc/Fc^+	E_{onset}^{OX} [a] (V) vs Fc/Fc^+	LUMO[b] (eV)	HOMO[b] (eV)	ΔE_{CV}[c] (eV)
C_{60} (pristine)	−0.97		−3.83		1.86 (lit.[91])
C_{60}-NH_2/NH_2 (**5**)	−1.05	+0.35	−3.75	−5.15	1.4
T_1-C_{60}-T_1 (**8**)	−1.05[d]	+0.66	−3.75	−5.46	1.7
T_2-C_{60}-T_2 (**9**)	−1.05[d]	+0.68	−3.75	−5.48	1.7
$(HT)_{13}$ (**11a′**)	−2.23	+0.33	−2.57	−5.13	2.6
$[C_{60}$-$(HT)_{13}]_n$ − $CHCl_3$ fraction	−2.19	+0.43	−2.61	−5.23	2.6
$(HT)_{28}$ (**11a**)	−2.19	+0.42	−2.61	−5.22	2.6
$[C_{60}$-$(HT)_{28}]_n$ − $CHCl_3$ fraction	−2.05	+0.44	−2.75	−5.24	2.5
$(OT)_{30}$ (**11b**)	−2.61	+0.37	−2.19	−5.17	3.0
$[C_{60}$-$(OT)_{30}]_n$ − $CHCl_3$ fraction	−2.11	+0.52	−2.69	−5.32	2.6
$[C_{60}$-$(OT)_{30}]_n$ − *o*-DCB fraction	−2.37	+0.54	−2.43	−5.34	2.9
$(DT)_{25}$ (**11c**)	−2.48	+0.26	−2.32	−5.06	2.7
$[C_{60}$-$(DT)_{25}]_n$ − $CHCl_3$ fraction	−2.24	+0.55	−2.56	−5.35	2.8
$[C_{60}$-$(DT)_{25}]_n$ − *o*-DCB fraction	−2.28	+0.52	−2.52	−5.32	2.8

[a] E_{onset}^{RED} and E_{onset}^{OX} are respectively the first onset reduction and oxidation potentials determined by CV. [b] The LUMO and HOMO values were calculated with respect to ferrocene (reference energy level = −4.8 eV below the vacuum level) according to the following equations:[92,93] LUMO = −[(E_{onset}^{RED} vs Fc/Fc^+) + 4.8] and HOMO = −[(E_{onset}^{OX} vs Fc/Fc^+) + 4.8]. [c] ΔE_{CV} is the calculated LUMO−HOMO difference. [d] Onset reduction potential of peak B (see Figure 14).

DOI: 10.1021/ma501788d
Macromolecules 2015, 48, 323−336

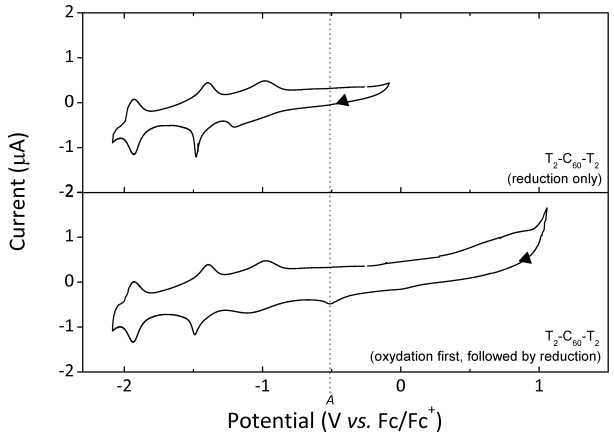

Figure 15. Differences in cyclic voltammograms according to the scanned potential window (T_2-C_{60}-T_2 model triad as example, casted films on Pt working electrode, measured in CH_3CN solution).

O3AT macromonomer are also reported. As shown in the example illustrated in Figure 16, the contribution of the fullerene moiety was not or very weakly detected on copolymers voltammograms. This is due to the small amount of C_{60} units related to the number of thiophene patterns inside O3AT units.

As a general trend, the oxidation and reduction of O3AT units were both shifted respectively to higher and lower potentials (in absolute value), when involved in copolymer structures. This results in lower HOMO and LUMO energy levels, while keeping closely similar gap values (ΔE_{CV}). As a consequence, $[C_{60}$-O3AT$]_n$ copolymers are less donor materials than their initial corresponding O3AT macromonomers.

3. CONCLUSION

In this work, a series of fullerene/oligothiophene alternating copolymers $[C_{60}$-O3AT$]_n$ were successfully synthesized by polycondensation. Several copolymers were designed using various alkyl chain and oligothiophene lengths. Prior to each synthesis, the operating conditions were first optimized using a cautious process of model polycondensation.

Each fullerene/oligothiophene copolymer was fractionated into two soluble fractions using a Soxhlet apparatus. The molecular weights of these fractions were limited due to a lack of solubility of higher polymerization degrees. According to NMR, GPC, and TGA analyses, it could be considered that their average compositions are O3AT-C_{60}-O3AT for chloroform soluble fractions and C_{60}-(O3AT-C_{60})$_2$ for *o*-dichlorobenzene soluble fractions.

According to cyclic voltammetry measurements, $[C_{60}$-O3AT$]_n$ copolymers are less donor materials than their initial corresponding O3AT macromonomers. However, the $[C_{60}$-O3AT$]_n$ copolymer family behave similarly to parent constituents in terms of light absorption.

Because of the covalent attachment of the fullerene acceptor to the conjugated donor polymer chain, which may enhance charge transfer, this new $[C_{60}$-O3AT$]_n$ copolymer family can be an interesting candidate for different use in organic photovoltaics. The investigation of its potential, as morphology compatibilizing or stabilizing agent, and as unique acceptor−donor material, is currently under progress.

4. EXPERIMENTAL SECTION

4.1. General Methods. *Nuclear magnetic resonance* analyses were performed using a Bruker Avance III/Ultrashield Plus 400 MHz spectrometer equipped with a 5 mm BBFO broadband probe. ^1H, ^{19}F, and ^{13}C frequencies were respectively 400.13, 376.46, and 100.62 MHz. The spectra were calibrated using the solvent residual peaks, and chemical shifts (δ) are expressed in parts per million (ppm). NMR multiplicities are reported by using the following abbreviations: s, singlet; d, doublet; t, triplet; q, quartet; m, multiplet; br, broad.

Infrared spectra were recorded at room temperature in attenuated total reflectance mode (ATR-FTIR) using a Nicolet 5700 FT-IR spectrometer.

Mass spectrometry analyses were performed using electrospray ionization time-of-flight (ESI-TOF) and matrix-assisted laser desorption ionization time-of-flight (MALDI-TOF) for molecules and polymers, respectively. ESI-TOF spectra were carried out on positive mode using an acceleration time-of-flight LCT WATERS mass spectrometer equipped with an electrospray ionization source. Samples were first dissolved in an adequate solvent and then diluted 80 times in methanol. The exact mass calibration was realized by internal calibration using *o*-phosphoric acid. For the MALDI-TOF experiments, a Voyager DE-STR/Applied Biosystems spectrometer was used. The polymer solutions were prepared in tetrahydrofuran (THF) at a concentration of 10 g/L and then mixed with a matrix solution (dithranol, 10 g/L in THF) in a 1/10 ratio. The final solutions were deposited onto an INOX target plate and allowed to dry in air at room temperature. The spectrometer was equipped with a nitrogen laser (λ = 337 nm), and the acquisitions were carried out using the reflectron positive ion mode.

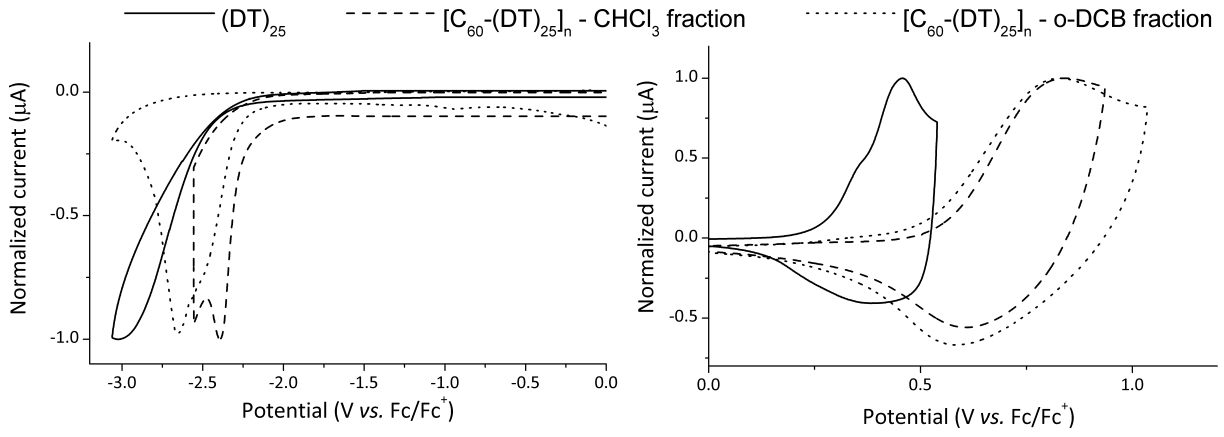

Figure 16. Cyclic voltammograms (right: oxidation; left: reduction) for the different fractions of $[C_{60}$-$(DT)_{25}]_n$ copolymer, compared to the initial $(DT)_{25}$ oligothiophene (casted films on Pt working electrode, measured in propylene carbonate solution).

DOI: 10.1021/ma501788d
Macromolecules 2015, 48, 323−336

Gel permeation chromatography analyses were conducted in two different conditions: at 25 °C in tetrahydrofuran and at 150 °C in 1,2,4-trichlorobenzene. The number-average (M_n) and weight-average (M_w) molecular weights and dispersities ($Đ = M_w/M_n$) are given in polystyrene equivalents (PS equiv). Room temperature GPC was carried out using a tripe detection chromatograph equipped with an Agilent 1200 Series isocratic pump, three Wyatt detectors (Viscostar at 25 °C, Optilab rEX at 658 nm−25 °C, Minidawn TREOS at 658 nm−5.7°−90°−134.3°), and a two PLgel MIXED-D columns set. Tetrahydrofuran at 25 °C was used as the mobile phase at a flow rate of 0.7 mL/min, and samples solutions were filtered through a 0.45 μm PTFE filter. High temperature GPC was carried out on a thermostated chromatograph equipped with a Waters GPCV2000 unity (pump, refractometric and viscometric detectors) and a three PLgel Olexis Guard columns set. Trichlorobenzene (stabilized by 0.2 g/L of butylhydroxytoluol) at 150 °C was used as the mobile phase at a flow rate of 1 mL/min, and samples solutions at 150 °C were prepared with the help of a Polymer Laboratories PL-SP260 high temperature sample preparation system during 2 h before to be filtered through a 1 μm PTFE filter and injected.

Thermogravimetric analysis measurements were performed using a METTLER TA2500 apparatus at a heating rate of 10 °C/min from 20 to 700 °C under a nitrogen atmosphere.

UV−visible spectra were recorded on a PerkinElmer Lambda 19 spectrometer. Solutions were as follow: 1.5×10^{-4} M in chloroform for triads and 0.1 mg/mL in *o*-dichlorobenzene for polymers, inside a 0.2 cm path length quartz cell. For solid-state measurements, a polymer solution (10 mg/mL in *o*-dichlorobenzene) was spin-coated on quartz plates.

Photoluminescence spectra were acquired on a Hitachi F-4500 fluorescence spectrophotometer using 1 cm path length quartz cells and polymers solutions in *o*-dichlorobenzene (~2×10^{-4} mg/mL). The fluorescence intensity of studied samples was independent of purging with inert gas so no precautions with regard to air were taken.

Electrochemical experiments were carried out with a Biologic SP-300 potentiostat. The cyclic voltammetry was performed in a three-electrode cell equipped with platinum working electrode (2.01 mm^2), platinum counter electrode, and Ag/Ag^+ reference electrode (silver wire in an acetonitrile solution of $AgNO_3$ (0.01 M) and TBAHFP (0.1 M)). Experiments were conducted in anhydrous and nitrogen-saturated 0.1 M tetrabutylammonium hexafluorophosphate (TBAHFP) solutions; either on compounds solutions (10^{-4} M for triads) or on films (polymer diluted solutions dropped and evaporated on the working electrode). Electrolyte solutions and scan rate conditions used were *o*-dichlorobenzene/acetonitrile: 95/5 at 100 mV s^{-1} for solutions and acetonitrile or propylene carbonate at 20 mV s^{-1} for films. The measured potentials were calibrated versus the ferrocene/ferrocenium couple ($E_{1/2}^{Fc/Fc^+}$) measured in the same experimental conditions.

4.2. Synthetic Details. C_{60} fullerene (99.5% purity) was purchased from SES Research, and PCBM (99.5% purity) from Nano-C. The aldehyde compounds **6** and **7** were synthesized using procedures close to those reported in the literature.[63,64] The 2-bromo-3-alkyl-5-iodothiopene derivatives (**10a**, **10b**, **10c**) were obtained according to a described procedure.[65] Other reagents were purchased from Sigma-Aldrich, Acros, or Fluka. All organic solvents used were of analytical or HPLC grade. Anhydrous diethyl ether, THF, and toluene were distilled over sodium/benzophenone prior to use. Dimethylformamide (DMF) was distilled over BaO and stored over molecular sieves.

All manipulations were performed under a dry nitrogen atmosphere using either magnetic (for molecules or oligomers) or mechanical (for copolymers) stirring. Purifications using column chromatography were performed using silica gel (60 Å, 70−200 μm).

*4,4′-(Trifluoroacetamido)benzophenone (**2**).* In a round-bottom flask under nitrogen, trifluoroacetic anhydride (66 mL, 478 mmol) and pyridine (~0.1 mL) were slowly added under stirring to a solution of 4,4′-diaminobenzophenone (**1**) (10.15 g, 47.8 mmol) in dry THF (250 mL). The mixture solution was stirred for 4 h at reflux. After cooling, the excess of trifluoroacetic anhydride was neutralized by a slow addition of methanol (30 mL) and water (30 mL). The resulting solution was extracted with dichloromethane (3 × 50 mL), the organic layer was dried over $MgSO_4$, and the solvent was evaporated under reduced pressure. The obtained solid was washed thoroughly with petroleum ether. After filtration, the solid was dried at 60 °C under vacuum to obtain **2** as white flakes; yield: 90%. ^{1}H NMR (400 MHz, acetone, δ, ppm): 10.53 (se, 2H, NH) ; 7.93 (d, ^3J = 8.6 Hz, 4H, aromatic) ; 7.86 (d, ^3J = 8.6 Hz, 4H, aromatic). ^{19}F NMR (376 MHz, acetone, δ, ppm): −76.21 (s, CF_3). ^{13}C NMR (100 MHz, acetone, δ, ppm): 194.19 (C═O); 156.18 + 155.81 ($^2J_{CF}$ = 37.4 Hz, C═O); 141.13 (aromatic C); 135.47 (aromatic C); 131.85 (aromatic CH); 121.10 (aromatic CH); 118.24 + 115.38 ($^1J_{CF}$ = 288.2 Hz, CF_3). MS (ESI): Calculated for $[C_{17}H_{10}F_6N_2O_3 + H]^+$: 405.0674. Found: 405.0668.

*4,4′-(Trifluoroacetamido)benzophenone-p-tosylhydrazone (**3**).* In a round-bottom flask under nitrogen, a solution of **2** (17.00 g, 42.08 mmol) and *p*-tosylhydrazide (7.84 g, 42.08 mmol) in dry toluene (200 mL) and absolute ethanol (17 mL) was stirred for 24 h at reflux. After cooling, the obtained precipitate was collected by filtration and washed thoroughly with petroleum ether. The solid was dried at 60 °C under vacuum to obtain **3** as a fine white powder; yield: 70%. ^{1}H NMR (400 MHz, MeOH, δ, ppm): 7.89 (d, ^3J = 8.3 Hz, 2H, aromatic); 7.85 (d, ^3J = 8.6 Hz, 2H, aromatic); 7.63 (d, ^3J = 8.8 Hz, 2H, aromatic); 7.44 (d, ^3J = 8.3 Hz, 2H, aromatic); 7.39 (d, ^3J = 8.8 Hz, 2H, aromatic); 7.30 (d, ^3J = 8.6 Hz, 2H, aromatic); 2.47 (s, 3H, CH_3). ^{19}F NMR (376 MHz, MeOH, δ, ppm): −76.20 (s, CF_3); −76.21 (s, CF_3). ^{13}C NMR (100 MHz, DMSO, δ, ppm): 157.14 + 156.77 ($^2J_{CF}$ = 37.4 Hz, C═O); 156.89 + 156.52 ($^2J_{CF}$ = 37.4 Hz, C═O); 154.84 (C═N); 145.50 (aromatic C); 139.15 (aromatic C); 137.31 (aromatic C); 135.94 (aromatic C); 132.19 (aromatic C); 130.96 (aromatic CH); 130.91 (aromatic C); 130.60 (aromatic CH); 129.50 (aromatic CH); 129.18 (aromatic CH); 122.66 (aromatic CH); 121.58 (aromatic CH); 118.79 + 115.94 ($^1J_{CF}$ = 288.2 Hz, CF_3); 118.76 + 115.91 ($^1J_{CF}$ = 288.2 Hz, CF_3); 21.53 (CH_3). MS (ESI): Calculated for $[C_{24}H_{18}F_6N_4O_4 + H]^+$: 573.1031. Found: 573.1025.

*4,4′-Aminobenzophenone-p-tosylhydrazone (**4**).* The previous compound **3** (12.87 g, 21.8 mmol) was dispersed in 100 mL of methanol and 100 mL of an aqueous solution of potassium carbonate (20% w/v) was added. After a few minutes of stirring, the entire compound **3** was dissolved, and the reaction mixture was allowed to react under stirring for 24 h at room temperature. The resulting solution was then extracted with dichloromethane (3 × 70 mL), the organic layer was dried over $MgSO_4$, and the solvent was evaporated under reduced pressure. The obtained beige solid (mixture of ionic and protonated forms) was eluted through a rapid silica gel chromatography (eluent: methanol, R_f = 0.70) to give **4** as a strong yellow fine powder; yield: 90%. ^{1}H NMR (400 MHz, DMSO, δ, ppm): 9.64 (s, 1H, NH); 7.78 (d, ^3J = 8.3 Hz, 2H, aromatic); 7.40 (d, ^3J = 8.3 Hz, 2H, aromatic); 6.95 (d, ^3J = 8.6 Hz, 2H, aromatic); 6.85 (d, ^3J = 8.4 Hz, 2H, aromatic); 6.61 (d, ^3J = 8.4 Hz, 2H, aromatic); 6.43 (d, ^3J = 8.6 Hz, 2H, aromatic); 5.45 (s, 2H, NH_2); 5.42 (s, 2H, NH_2); 2.39 (s, 3H, CH_3). ^{13}C NMR (100 MHz, DMSO, δ, ppm): 156.74 (C═N); 150.25 (C−NH_2); 149.59 (C−NH_2); 142.92 (aromatic C); 136.27 (aromatic C); 130.08 (aromatic CH); 129.18 (aromatic CH); 129.00 (aromatic CH); 127.83 (aromatic CH); 129.21 (aromatic C); 119.53 (aromatic C); 113.17 (aromatic CH); 112.86 (aromatic CH); 21.03 (CH_3). MS (ESI): Calculated for $[C_{20}H_{20}N_4O_2S + H]^+$: 381.1. Found: 381.1.

*[6,6]-Bis(4-aminophenyl)methanofullerene (**5**).* In a round-bottom flask under nitrogen, the previous compound **4** (2.00 g, 5.05 mmol) was dissolved in 100 mL of anhydrous pyridine, and 27.30 mg (5.05 mmol) of sodium methoxide was added all at once. The mixture solution was stirred for 15 min at room temperature. Then, a solution of fullerene C_{60} (2.55 g, 3.54 mmol) in 250 mL of *o*-dichlorobenzene (previously filled by nitrogen using three freeze−pump−thaw cycles) was added to the reaction medium. This reaction mixture was stirred for 18 h at reflux in the dark. After cooling, the solvents were evaporated under reduced pressure (under a fume cupboard). The obtained solid was purified by silica gel chromatography to give

DOI: 10.1021/ma501788d
Macromolecules 2015, 48, 323−336

residual C_{60} (eluent: toluene, R_f = 1) and compound **5** (eluent: toluene/ethyl acetate 8/2, R_f = 0.28). The final product was dried at 100 °C under vacuum during 48 h to give **5** as a fine brown powder always containing 5−10% of residual toluene (^{1}H NMR determination); yield: 20%. ^{1}H NMR (400 MHz, DMSO/CF_3COOD, δ, ppm): 8.56 (d, ^3J = 8.4 Hz, 2H, aromatic); 7.52 (d, ^3J = 8.4 Hz, 2H, aromatic). ^{13}C NMR (100 MHz, DMSO/CF_3COOD, δ, ppm): 148.45; 145.92; 144.99; 144.93; 144.45; 144.27; 144.11; 143.61; 142.77; 142.67; 141.91; 141.79; 140.44; 138.75 (aromatic C); 137.30; 132.70 (aromatic CH); 131.88 (aromatic C); 124.02 (aromatic CH); 78.85 (C_{60} sp^3 C); 56.48 (bridge C). MS (ESI): Calculated for $[C_{73}H_{12}N_2]^{\bullet+}$: 916.1000. Found: 916.0990.

General Procedure for the Synthesis of Model Triads T_n-C_{60}-T_n. In a dried round-bottom flask under nitrogen, compound **5** (99.22 mg, 0.11 mmol) and an excess of aldehyde (**6** or **7**, 0.97 mmol) were introduced in 30 mL of *m*-cresol. The reaction mixture was stirred for 24 h at 60 °C. At the end of the reaction, the *m*-cresol and excess of aldehyde were eliminated using a Kugelrohr distillation apparatus (100 °C, 0.67 mbar). The obtained solid was washed thoroughly with methanol, collected by filtration, and purified by extraction using chloroform. The solution was concentrated under reduced pressure, and the final product dried at 60 °C under vacuum during 24 h to give the desired triad.

8. Fine brown powder, yield: 70%. ^{1}H NMR (400 MHz, $CDCl_3$, δ, ppm): 8.67 (s, 2H, Schiff base); 8.13 (d, ^3J = 8.3 Hz, 4H, phenyl); 7.42 (d, ^3J = 5 Hz, 2H, thiophene); 7.31 (d, ^3J = 8.3 Hz, 4H, phenyl); 6.94 (d, ^3J = 5 Hz, 2H, thiophene); 2.84 (t, ^3J = 7.6 Hz, 4H, αCH_2); 1.65 (q, ^3J = 7.4 Hz, 4H, βCH_2); 1.41−1.27 (m, 12H, aliph CH_2); 0.88 (t, 6H, aliph CH_3). ^{13}C NMR (100 MHz, $C_2D_2Cl_4$, δ, ppm): 152.17 (Schiff base); 151.21; 148.44; 147.95; 145.18; 144.97; 144.90; 144.49; 144.45; 144.06; 143.62; 142.86; 142.78; 142.11; 142.08; 141.91; 140.65; 137.99; 136.18; 135.97; 131.72; 130.11; 121.37; 78.92 (C_{60} sp^3 C); 77.32 (C_{60} sp^3 C); 57.19 (bridge C); 31.51; 31.17; 28.94; 28.51; 22.52; 14.09.

9. Fine brown powder, yield: 70%. ^{1}H NMR (400 MHz, $CDCl_3$, δ, ppm): 8.65 (s, 2H, Schiff base); 8.13 (d, ^3J = 8.3 Hz, 4H, phenyl); 7.33 (d, ^3J = 8.3 Hz, 4H, phenyl); 7.20 (d, ^3J = 5.2 Hz, 2H, thiophene); 6.99 (s, 2H, thiophene); 6.94 (d, ^3J = 5.2 Hz, 2H, thiophene); 2.83 (t, ^3J = 7.7 Hz, 8H, αCH_2); 1.71−1.61 (m, 8H, βCH_2); 1.44−1.27 (m, 24H, aliph CH_2); 0.95−0.82 (m, 12H, aliph CH_3). ^{13}C NMR (100 MHz, $CDCl_3$, δ, ppm): 151.98 (Schiff base); 151.77; 148.73; 148.40; 145.52; 145.34; 145.17; 144.87; 144.79; 144.45; 144.00; 143.25; 143.18; 143.09; 142.40; 142.27; 141.07; 141.03; 138.42; 136.47; 135.74; 131.90; 130.68; 130.56; 128.35; 124.67; 121.68; 79.33 (C_{60} sp^3 C); 77.87 (C_{60} sp^3 C); 57.70 (bridge C); 31.84; 31.79; 31.41; 30.62; 29.62; 29.35; 29.20; 28.78; 22.76; 22.74; 14.23.

General Procedure for the Synthesis of Dicarbonylated Oligothiophenes. In a dried round-bottom flask under nitrogen, a 3-alkyl-5-iodothiopene derivative (**10a-b-c**, 34.44 mmol) was dissolved in 100 mL of fresh distilled THF and cooled down to 0 °C. Then, a 1.6 M *tert*-butylmagnesium chloride solution in THF (14.5 mL, 35 mmol) was added dropwise, and the reaction mixture was stirred for 2h at 0 °C. A quantity of 1,3-bis(diphenylphosphino)propane nickel(II) chloride [Ni(dppp)Cl_2] was then added in accordance to the desired degree of polymerization. The reaction mixture was stirred for 4 h at room temperature. The resulting solution was diluted by addition of 200 mL of anhydrous THF and quenched with 20 mL of a 2 M hydrochloric acid aqueous solution. After 30 min of stirring, the organic layer was extracted with chloroform (3 × 100 mL), washed with water (2 × 100 mL), and dried over $MgSO_4$. The polymer was collected by solvent evaporation under reduced pressure and purified using Soxhlet extraction with methanol, petroleum ether, and chloroform, sequentially. The concentrated chloroform fraction was collected and dried overnight under reduced pressure to obtain the corresponding oligo-3-alkylthiophene O3AT terminated either by H or Br; yield: 70−80%.

To convert the previous O3AT-H/Br into a fully proton terminated oligothiophene, the polymer was dissolved in 100 mL of anhydrous THF (at 60 °C if necessary) under nitrogen. Then, 10 mL of a 1.6 M $LiAlH_4$ solution in THF was added at room temperature, and the reaction was allowed to stir for 12 h. The reaction was quenched by adding 1 mL of water, 1 mL of NaOH aqueous solution (15 wt %), and 3 mL of water. The reaction mixture was then diluted in 300 mL of chloroform, and a white precipitate was eliminated by filtration. The organic layer was separated, washed with water, dried over $MgSO_4$, and concentrated under reduced pressure. The obtained blackish-green solid was dried overnight under reduced pressure to give O3AT H/H terminated (**11**); yield: 90−95%.

To convert O3AT-H/H into the dialdehyde-terminated oligothiophene, the Vilsmeier reagent was first formed *in situ*. In a dried round-bottom flask under nitrogen, $POCl_3$ (1 mL, 10.7 mmol) was added dropwise to anhydrous DMF (1 mL, 12.9 mmol) at room temperature. The solution is allowed to stir for 3 h until getting a red complex typical of the Vilsmeier reagent. In another dried round-bottom flask under nitrogen, the previous O3AT-H/H was dissolved (at 60 °C if necessary) in 100 mL of dichloromethane (dried on molecular sieve), and the Vilsmeier reagent was transferred dropwise at room temperature. The reaction mixture was stirred for 5 days at 60 °C. Then, after cooling to room temperature, 100 mL of sodium acetate saturated aqueous solution was added. The reaction mixture was allowed to stir for 6−24 h until getting a fluorescent solution. The resulting solution was extracted with chloroform (3 × 50 mL), washed with water, and dried over $MgSO_4$. The polymer was collected by solvent concentration under reduced pressure, precipitation in methanol, and purification using Soxhlet extraction with methanol and chloroform, sequentially. The concentrated chloroform fraction was then collected and again precipitated in methanol before to be dried 24 h at 60 °C under reduced pressure to obtain O3AT CHO/CHO terminated (**12**) as blackish-green powder; yield: 90−97%.

11. General O3AT-H/H ^{1}H NMR profile (400 MHz, $CDCl_3$, δ, ppm, *minor peaks in italics*): 6.98 (br s, arom H); *6.90 (br s, end arom H)*; 2.80 (br t, αCH_2); *2.61 (t, end αCH_2)*; 1.75−1.60 (br m, βCH_2); 1.50−1.20 (br m, CH_2); 1.00−0.80 (br m, CH_3).

12. General O3AT-CHO/CHO ^{1}H NMR profile (400 MHz, $CDCl_3$, δ, ppm, *minor peaks in italics*): *10.01 + 9.98 (2s, CHO cis + trans)*; *7.05 (br s, end arom H)*; 6.98 (br s, arom H); *2.95 (t, end αCH_2)*; 2.80 (br t, αCH_2); 1.75−1.60 (br m, βCH_2); 1.50−1.20 (br m, CH_2); 1.00−0.80 (br m, CH_3).

General Procedure for the Synthesis of Model Copolymers [ODA-O3AT]$_n$: Study of the Optimal ODA/O3AT Ratio. In a dried glass reactor equipped with mechanical stirring, 250 mg of O3AT-CHO/CHO (**12**) was dissolved in 6 mL of anhydrous THF. 2 mg of PTSA (catalyst) and a spatula of $CaCl_2$ (internal drying agent) were added to the solution. In another flask, a solution of 4,4′-oxidianiline ODA (2 g) dissolved in 50 mL of anhydrous DMF was prepared. Then, a series of polycondensation was realized by introducing into the reactor various quantities of the prepared ODA solution (from 0.1 to 1 mL) with an additional volume of DMF in order to keep a 6/2 THF/DMF ratio. The reaction mixture was stirred for 24 h at 55 °C. At the end of the reaction, a sample of the crude reaction mixture was taken for ^{1}H NMR analysis. For the optimal ODA/O3AT ratio, determined by ^{1}H NMR, the remaining solution was concentrated under reduced pressure and purified using Soxhlet extraction with methanol, petroleum ether, and chloroform, sequentially. The concentrated chloroform fraction was then collected to obtain [ODA-O3AT]$_n$ copolymer (**13**) as a blackish-green solid.

13. General [ODA-O3AT]$_n$ ^{1}H NMR profile (400 MHz, $C_2D_2Cl_4$, 70 °C, δ, ppm): 8.65 (br s, Schiff base); 7.30 (br d, phenyl); 7.10 (br d, phenyl); 7.03 (br s, thiophene); 2.85 (m, αCH_2); 1.85−1.65 (br m, βCH_2); 1.60−1.25 (br m, CH_2); 1.05−0.85 (br m, CH_3); possible minor peaks corresponding to end-chain units are not detailed (see Figure 10).

General Procedure for the Synthesis of Copolymers [C_{60}-O3AT]$_n$. In a dried glass reactor equipped with mechanical stirring, 250 mg of O3AT-CHO/CHO (**12**) was dissolved in 12 mL of anhydrous THF. 2 mg of PTSA (catalyst) and a spatula of $CaCl_2$ (internal drying agent) were added to the solution. In another flask, compound **5** (C_{60}-NH_2/NH_2, 0.11 mmol for **12a**, 0.05 mmol for **12a′**, 0.04 mmol for **12b** and **12c**) was dissolved in 4 mL of anhydrous DMF. This solution was degassed by nitrogen bubbling and introduced into the reactor,

DOI: 10.1021/ma501788d
Macromolecules 2015, 48, 323−336

previously protected from light. The reaction mixture was stirred for 7 days at 55 °C in the dark. At the end of the reaction, the solution was concentrated under reduced pressure and purified using Soxhlet extraction with methanol, petroleum ether, chloroform, and *o*-dichlorobenzene, sequentially. The concentrated chloroform and *o*-dichlorobenzene fractions were then collected and dried 24 h under reduced pressure to obtain two blackish-green fractions of the $[C_{60}\text{-O3AT}]_n$ copolymer (**14**).

14. General $[C_{60}\text{-O3AT}]_n$ ^{1}H NMR profile (400 MHz, $C_2D_2Cl_4$, 70 °C, δ, ppm, *peaks in italics representative of the C_{60} building block as end-chain unit can be not detectable in some fractions)*: 10.03 + 10.01 (2s, CHO cis + trans); 8.72 (br s, Schiff base); 8.18 (br d, phenyl); *8.11 (br, end phenyl)*; *7.78 (br, end phenyl)*; 7.37 (br d, phenyl); *7.25 (br, end phenyl)*; 7.03 (br s, thiophene); *6.80 (br, end phenyl)*; 2.85 (m, αCH_2); 1.85−1.65 (br m, βCH_2); 1.60−1.25 (br m, CH_2); 1.05−0.85 (br m, CH_3).

AUTHOR INFORMATION

Corresponding Author

*E-mail lara.perrin@univ-savoie.fr (L.P.).

Present Address

R.M.: CNRS, UMR 5223, Ingénierie des Matériaux Polymères, F-69622 Villeurbanne Cedex, France.

Notes

The authors declare no competing financial interest.

ACKNOWLEDGMENTS

The authors thank Prof. Lionel Flandin for fruitful discussions and Vincent Martin for GPC characterizations. The authors also thank Dr. Martial Billon from INAC/SPrAM/CREAB (UMR 5819 CEA-CNRS-UJF) for useful discussions on cyclic voltammetry measurements and Dr. Noëlla Lemaitre from CEA/LITEN/INES for availability of fluorescence spectroscopy measurements. The Institut National de l'Energie Solaire (INES) and the financial support from Assemblée des Pays de Savoie, Centre National de la Recherche Scientifique, and Commissariat à l'énergie atomique et aux énergies alternatives are gratefully acknowledged.

REFERENCES

(1) Chamberlain, G. A. *Sol. Cells* **1983**, *8* (1), 47−83.
(2) Merritt, V. Y.; Hovel, H. J. *Appl. Phys. Lett.* **1976**, *29* (7), 414−415.
(3) Morel, D. L.; Ghosh, A. K.; Feng, T.; Stogryn, E. L.; Purwin, P. E.; Shaw, R. F.; Fishman, C. *Appl. Phys. Lett.* **1978**, *32* (8), 495−497.
(4) Krebs, F. C.; Spanggard, H.; Kjær, T.; Biancardo, M.; Alstrup, J. *Mater. Sci. Eng., B* **2007**, *138* (2), 106−111.
(5) Espinosa, N.; Hosel, M.; Angmo, D.; Krebs, F. C. *Energy Environ. Sci.* **2012**, *5* (1), 5117−5132.
(6) Dang, M. T.; Hirsch, L.; Wantz, G. *Adv. Mater.* **2011**, *23* (31), 3597−3602.
(7) Reyes-Reyes, M.; Kim, K.; Dewald, J.; López-Sandoval, R.; Avadhanula, A.; Curran, S.; Carroll, D. L. *Org. Lett.* **2005**, *7* (26), 5749−5752.
(8) Green, M. A.; Emery, K.; Hishikawa, Y.; Warta, W.; Dunlop, E. D. *Prog. Photovoltaics* **2014**, *22* (7), 701−710.
(9) You, J.; Dou, L.; Yoshimura, K.; Kato, T.; Ohya, K.; Moriarty, T.; Emery, K.; Chen, C.-C.; Gao, J.; Li, G.; Yang, Y. *Nat. Commun.* **2013**, *4*, 1446.
(10) Xu, T.; Yu, L. *Mater. Today* **2014**, *17* (1), 11−15.
(11) Hoppe, H.; Sariciftci, N. S. *J. Mater. Chem.* **2006**, *16* (1), 45−61.
(12) Ray, B.; Alam, M. A. *Sol. Energy Mater. Sol. Cells* **2012**, *99* (0), 204−212.
(13) Shaw, P. E.; Ruseckas, A.; Samuel, I. D. W. *Adv. Mater.* **2008**, *20* (18), 3516−3520.
(14) Drummy, L. F.; Davis, R. J.; Moore, D. L.; Durstock, M.; Vaia, R. A.; Hsu, J. W. P. *Chem. Mater.* **2011**, *23* (3), 907−912.
(15) Sariciftci, N. S. *J. Mater. Chem.* **2006**, *16* (1), 45−61.
(16) Müller, C.; Ferenczi, T. A. M.; Campoy-Quiles, M.; Frost, J. M.; Bradley, D. D. C.; Smith, P.; Stingelin-Stutzmann, N.; Nelson, J. *Adv. Mater.* **2008**, *20* (18), 3510−3515.
(17) Abbas, M.; Tekin, N. *Appl. Phys. Lett.* **2012**, *101* (7), 073302−4.
(18) Janssen, G.; Aguirre, A.; Goovaerts, E.; Vanlaeke, P.; Poortmans, J.; Manca, J. *Eur. Phys. J.: Appl. Phys.* **2007**, *37* (03), 287−290.
(19) Song, J.; Du, C.; Li, C.; Bo, Z. *J. Polym. Sci., Part A: Polym. Chem.* **2011**, *49* (19), 4267−4274.
(20) Hoven, C. V.; Dang, X.-D.; Coffin, R. C.; Peet, J.; Nguyen, T.-Q.; Bazan, G. C. *Adv. Mater.* **2010**, *22* (8), E63−E66.
(21) Lee, J. K.; Ma, W. L.; Brabec, C. J.; Yuen, J.; Moon, J. S.; Kim, J. Y.; Lee, K.; Bazan, G. C.; Heeger, A. J. *J. Am. Chem. Soc.* **2008**, *130* (11), 3619−3623.
(22) Miller, S.; Fanchini, G.; Lin, Y.-Y.; Li, C.; Chen, C.-W.; Su, W.-F.; Chhowalla, M. *J. Mater. Chem.* **2008**, *18* (3), 306−312.
(23) Verploegen, E.; Miller, C. E.; Schmidt, K.; Bao, Z.; Toney, M. F. *Chem. Mater.* **2012**, *24* (20), 3923−3931.
(24) Ma, W.; Yang, C.; Gong, X.; Lee, K.; Heeger, A. J. *Adv. Funct. Mater.* **2005**, *15* (10), 1617−1622.
(25) Sivula, K.; Ball, Z. T.; Watanabe, N.; Fréchet, J. M. J. *Adv. Mater.* **2006**, *18* (2), 206−210.
(26) Tsai, J.-H.; Lai, Y.-C.; Higashihara, T.; Lin, C.-J.; Ueda, M.; Chen, W.-C. *Macromolecules* **2010**, *43* (14), 6085−6091.
(27) Gernigon, V.; Lévêque, P.; Brochon, C.; Audinot, J.-N.; Leclerc, N.; Bechara, R.; Richard, F.; Heiser, T.; Hadziioannou, G. *Eur. Phys. J.: Appl. Phys.* **2011**, *56* (03), 34107/1−6.
(28) Goubard, F.; Wantz, G. *Polym. Int.* **2014**, *63* (8), 1362−1367.
(29) Dang, M. T.; Hirsch, L.; Wantz, G.; Wuest, J. D. *Chem. Rev.* **2013**, *113* (5), 3734−3765.
(30) Yuan, K.; Chen, L.; Chen, Y. *Polym. Int.* **2014**, *63* (4), 593−606.
(31) Topham, P. D.; Parnell, A. J.; Hiorns, R. C. *J. Polym. Sci., Part B: Polym. Phys.* **2011**, *49* (16), 1131−1156.
(32) Yang, C.; Lee, J. K.; Heeger, A. J.; Wudl, F. *J. Mater. Chem.* **2009**, *19* (30), 5416−5423.
(33) Yassar, A.; Miozzo, L.; Gironda, R.; Horowitz, G. *Prog. Polym. Sci.* **2013**, *38* (5), 791−844.
(34) Economopoulos, S. P.; Chochos, C. L.; Gregoriou, V. G.; Kallitsis, J. K.; Barrau, S.; Hadziioannou, G. *Macromolecules* **2007**, *40* (4), 921−927.
(35) Lai, Y.-C.; Higashihara, T.; Hsu, J.-C.; Ueda, M.; Chen, W.-C. *Sol. Energy Mater. Sol. Cells* **2012**, *97* (0), 164−170.
(36) Lee, J. U.; Jung, J. W.; Emrick, T.; Russell, T. P.; Jo, W. H. *J. Mater. Chem.* **2010**, *20* (16), 3287−3294.
(37) Raja, R.; Liu, W.-S.; Hsiow, C.-Y.; Hsieh, Y.-J.; Rwei, S.-P.; Chiu, W.-Y.; Wang, L. *Org. Electron.* **2014**, *15* (10), 2223−2233.
(38) Kim, J. B.; Allen, K.; Oh, S. J.; Lee, S.; Toney, M. F.; Kim, Y. S.; Kagan, C. R.; Nuckolls, C.; Loo, Y.-L. *Chem. Mater.* **2010**, *22* (20), 5762−5773.
(39) Dai, C.-A.; Dair, B. J.; Dai, K. H.; Ober, C. K.; Kramer, E. J.; Hui, C.-Y.; Jelinski, L. W. *Phys. Rev. Lett.* **1994**, *73* (18), 2472−2475.
(40) Lee, M. S.; Lodge, T. P.; Macosko, C. W. *J. Polym. Sci., Part B: Polym. Phys.* **1997**, *35* (17), 2835−2842.
(41) Cravino, A.; Zerza, G.; Maggini, M.; Bucella, S.; Svensson, M.; Andersson, M. R.; Neugebauer, H.; Sariciftci, N. S. *Chem. Commun.* **2000**, *24*, 2487−2488.
(42) Nourdine, A.; Perrin, L.; de Bettignies, R.; Guillerez, S.; Flandin, L.; Alberola, N. *Polymer* **2011**, *52* (26), 6066−6073.
(43) Perrin, L.; Nourdine, A.; Planes, E.; Carrot, C.; Alberola, N.; Flandin, L. *J. Polym. Sci., Part B: Polym. Phys.* **2013**, *51* (4), 291−302.
(44) Aldea, G.; Chitanu, G. C.; Delaunay, J.; Nunzi, J.-M.; Simionescu, B. C.; Cousseau, J. *J. Polym. Sci., Part A: Polym. Chem.* **2005**, *43* (23), 5814−5822.
(45) Adamopoulos, G.; Heiser, T.; Giovanella, U.; Ould-Saad, S.; van de Wetering, K. I.; Brochon, C.; Zorba, T.; Paraskevopoulos, K. M.; Hadziioannou, G. *Thin Solid Films* **2006**, *511−512*, 371−376.
(46) Hawker, C. J. *Macromolecules* **1994**, *27* (17), 4836−4837.

DOI: 10.1021/ma501788d
Macromolecules 2015, 48, 323−336

(47) Heuken, M.; Komber, H.; Voit, B. *Macromol. Chem. Phys.* **2012**, *213* (1), 97−107.
(48) Ferraris, J. P.; Yassar, A.; Loveday, D. C.; Hmyene, M. *Opt. Mater.* **1998**, *9* (1−4), 34−42.
(49) Palermo, E. F.; Darling, S. B.; McNeil, A. J. *J. Mater. Chem. C* **2014**, *2* (17), 3401−3406.
(50) Hiorns, R. C.; Cloutet, E.; Ibarboure, E.; Khoukh, A.; Bejbouji, H.; Vignau, L.; Cramail, H. *Macromolecules* **2010**, *43* (14), 6033−6044.
(51) Hiorns, R. C.; Cloutet, E.; Ibarboure, E.; Vignau, L.; Lemaitre, N.; Guillerez, S.; Absalon, C.; Cramail, H. *Macromolecules* **2009**, *42* (10), 3549−3558.
(52) Camp, A. G.; Lary, A.; Ford, W. T. *Macromolecules* **1995**, *28* (23), 7959−7961.
(53) Zhihua, L.; Goh, S. H.; Lee, S. Y.; Sun, X.; Ji, W. *Polymer* **1999**, *40* (10), 2863−2867.
(54) Hiorns, R. C.; Iratçabal, P.; Bégué, D.; Khoukh, A.; De Bettignies, R.; Leroy, J.; Firon, M.; Sentein, C.; Martinez, H.; Preud'homme, H.; Dagron-Lartigau, C. *J. Polym. Sci., Part A: Polym. Chem.* **2009**, *47* (9), 2304−2317.
(55) Roncali, J. *Chem. Soc. Rev.* **2005**, *34* (6), 483−495.
(56) Giacalone, F.; Martin, N. *Chem. Rev.* **2006**, *106* (12), 5136−5190.
(57) Sijbesma, R.; Srdanov, G.; Wudl, F.; Castoro, J. A.; Wilkins, C.; Friedman, S. H.; DeCamp, D. L.; Kenyon, G. L. *J. Am. Chem. Soc.* **1993**, *115* (15), 6510−6512.
(58) Richardson, C. F.; Schuster, D. I.; Wilson, S. R. *Org. Lett.* **2000**, *2* (8), 1011−1014.
(59) Marcorin, G. L.; Da Ros, T.; Castellano, S.; Stefancich, G.; Bonin, I.; Miertus, S.; Prato, M. *Org. Lett.* **2000**, *2* (25), 3955−3958.
(60) Gómez, R.; Segura, J. L.; Martín, N. *Org. Lett.* **2005**, *7* (4), 717−720.
(61) Prato, M.; Lucchini, V.; Maggini, M.; Stimpfl, E.; Scorrano, G.; Eiermann, M.; Suzuki, T.; Wudl, F. *J. Am. Chem. Soc.* **1993**, *115* (18), 8479−8480.
(62) Guldi, D. M.; Hungerbühler, H.; Carmichael, I.; Asmus, K.-D.; Maggini, M. *J. Phys. Chem. A* **2000**, *104* (38), 8601−8608.
(63) Bronstein, H.; Hurhangee, M.; Fregoso, E. C.; Beatrup, D.; Soon, Y. W.; Huang, Z.; Hadipour, A.; Tuladhar, P. S.; Rossbauer, S.; Sohn, E.-H.; Shoaee, S.; Dimitrov, S. D.; Frost, J. M.; Ashraf, R. S.; Kirchartz, T.; Watkins, S. E.; Song, K.; Anthopoulos, T.; Nelson, J.; Rand, B. P.; Durrant, J. R.; McCulloch, I. *Chem. Mater.* **2013**, *25* (21), 4239−4249.
(64) Weidelener, M.; Wessendorf, C. D.; Hanisch, J.; Ahlswede, E.; Gotz, G.; Linden, M.; Schulz, G.; Mena-Osteritz, E.; Mishra, A.; Bauerle, P. *Chem. Commun.* **2013**, *49* (92), 10865−10867.
(65) Loewe, R. S.; Ewbank, P. C.; Liu, J.; Zhai, L.; McCullough, R. D. *Macromolecules* **2001**, *34* (13), 4324−4333.
(66) Iovu, M. C.; Sheina, E. E.; Gil, R. R.; McCullough, R. D. *Macromolecules* **2005**, *38* (21), 8649−8656.
(67) Miyakoshi, R.; Yokoyama, A.; Yokozawa, T. *J. Am. Chem. Soc.* **2005**, *127* (49), 17542−17547.
(68) Cremer, J.; Mena-Osteritz, E.; Pschierer, N. G.; Mullen, K.; Bauerle, P. *Org. Biomol. Chem.* **2005**, *3* (6), 985−995.
(69) Miyakoshi, R.; Yokoyama, A.; Yokozawa, T. *Macromol. Rapid Commun.* **2004**, *25* (19), 1663−1666.
(70) Hiorns, R. C.; Khoukh, A.; Gourdet, B.; Dagron-Lartigau, C. *Polym. Int.* **2006**, *55* (6), 608−620.
(71) Liu, J.; McCullough, R. D. *Macromolecules* **2002**, *35* (27), 9882−9889.
(72) Bidan, G.; De Nicola, A.; Enée, V.; Guillerez, S. *Chem. Mater.* **1998**, *10* (4), 1052−1058.
(73) Barbarella, G.; Bongini, A.; Zambianchi, M. *Macromolecules* **1994**, *27* (11), 3039−3045.
(74) Netopilík, M.; Kratochvíl, P. *Polymer* **2003**, *44* (12), 3431−3436.
(75) Holdcroft, S. *J. Polym. Sci., Part B: Polym. Phys.* **1991**, *29* (13), 1585−1588.
(76) Liu, J.; Loewe, R. S.; McCullough, R. D. *Macromolecules* **1999**, *32* (18), 5777−5785.
(77) Rashidzadeh, H.; Guo, B. *Anal. Chem.* **1998**, *70* (1), 131−135.
(78) Nielen, M. W. F. *Mass Spectrom. Rev.* **1999**, *18* (5), 309−344.
(79) Audouin, F.; Nuffer, R.; Mathis, C. *J. Polym. Sci., Part A: Polym. Chem.* **2004**, *42* (14), 3456−3463.
(80) Hare, J. P.; Kroto, H. W.; Taylor, R. *Chem. Phys. Lett.* **1991**, *177* (4−5), 394−398.
(81) Otsubo, T.; Aso, Y.; Takimiya, K. *J. Mater. Chem.* **2002**, *12* (9), 2565−2575.
(82) van Hal, P. A.; Knol, J.; Langeveld-Voss, B. M. W.; Meskers, S. C. J.; Hummelen, J. C.; Janssen, R. A. J. *J. Phys. Chem. A* **2000**, *104* (25), 5974−5988.
(83) Narutaki, M.; Takimiya, K.; Otsubo, T.; Harima, Y.; Zhang, H.; Araki, Y.; Ito, O. *J. Org. Chem.* **2006**, *71* (5), 1761−1768.
(84) Baffreau, J.; Perrin, L.; Leroy-Lhez, S.; Hudhomme, P. *Tetrahedron Lett.* **2005**, *46* (27), 4599−4603.
(85) Boudouris, B. W.; Molins, F.; Blank, D. A.; Frisbie, C. D.; Hillmyer, M. A. *Macromolecules* **2009**, *42* (12), 4118−4126.
(86) Negishi, N.; Takimiya, K.; Otsubo, T.; Harima, Y.; Aso, Y. *Chem. Lett.* **2004**, *33* (6), 654−655.
(87) Negishi, N.; Takimiya, K.; Otsubo, T.; Harima, Y.; Aso, Y. *Synth. Met.* **2005**, *152* (1−3), 125−128.
(88) Xie, Q.; Arias, F.; Echegoyen, L. *J. Am. Chem. Soc.* **1993**, *115* (21), 9818−9819.
(89) Echegoyen, L.; Echegoyen, L. E. *Acc. Chem. Res.* **1998**, *31* (9), 593−601.
(90) Cravino, A.; Zerza, G.; Neugebauer, H.; Maggini, M.; Bucella, S.; Menna, E.; Svensson, M.; Andersson, M. R.; Brabec, C. J.; Sariciftci, N. S. *J. Phys. Chem. B* **2001**, *106* (1), 70−76.
(91) Rabenau, T.; Simon, A.; Kremer, R. K.; Sohmen, E. *Z. Phys. B: Condens. Matter* **1993**, *90* (1), 69−72.
(92) Pommerehne, J.; Vestweber, H.; Guss, W.; Mahrt, R. F.; Bässler, H.; Porsch, M.; Daub, J. *Adv. Mater.* **1995**, *7* (6), 551−554.
(93) Cardona, C. M.; Li, W.; Kaifer, A. E.; Stockdale, D.; Bazan, G. C. *Adv. Mater.* **2011**, *23* (20), 2367−2371.

DOI: 10.1021/ma501788d
Macromolecules 2015, 48, 323−336